

Phylogenetic comparisons between Type IX Secretion System (T9SS) protein components suggest evidence of horizontal gene transfers

Reeki Emrizal¹, Nor Azlan Nor Muhammad^{Corresp. 1}

¹ Centre for Bioinformatics Research, Institute of Systems Biology, Universiti Kebangsaan Malaysia, Bangi, Selangor, Malaysia

Corresponding Author: Nor Azlan Nor Muhammad
Email address: norazlanm@ukm.edu.my

Porphyromonas gingivalis is one of the major bacteria that causes periodontitis. Chronic periodontitis is a severe form of periodontal disease that ultimately lead to tooth loss. Virulence factors that contribute to periodontitis are secreted by Type IX Secretion System (T9SS). There are aspects of T9SS protein components that have yet to be characterised. Thus, the aim of this study is to investigate phylogenetic relationship between members of 20 T9SS component protein families. The Bayesian Inference (BI) trees for 19 T9SS protein components exhibit monophyletic clades for all major classes under Bacteroidetes with a strong support for the monophyletic clades or its subclades that is consistent with phylogeny exhibited by the constructed BI tree of 16S rRNA. The BI tree of PorR is different from the 19 BI trees of T9SS protein components as it does not exhibit monophyletic clades for all major classes under Bacteroidetes. There is a strong support for the phylogeny exhibited by BI tree of PorR deviates from the phylogeny based on 16S rRNA. Hence, it is possible that *porR* gene is subjected to horizontal transfer as it is known that virulence factor gene could be horizontally transferred. Seven genes (*porR* included) that involved in the biosynthesis of A-LPS are found to be flanked by insertion sequences (IS5 family transposons). Therefore, the intervening DNA segment that contains *porR* gene might be transposed and subjected to conjugative transfer. Thus, the seven genes can be co-transferred via horizontal gene transfer. The BI tree of UgdA does not exhibit monophyletic clades for all major classes under Bacteroidetes which is similar to the BI tree of PorR (both are a part of the seven genes). Both BI trees also exhibit similar topology as the four identified clusters with a strong support have similar relative positions to each other in both BI trees. This reinforces the possibility that *porR* and the other six genes might be horizontally transferred. Other than the BI tree of PorR, the other 19 BI trees of T9SS protein components also exhibit evidence of horizontal gene transfer. However their genes might undergo horizontal gene transfer less frequently compared to *porR* because the intervening DNA segment that contains *porR* is easily exchanged

between bacteria under Bacteroidetes due to the presence of insertion sequences (IS5 family transposons) that flanking it. In conclusion, this study can provide a better understanding about the phylogeny of T9SS protein components.

1 **Phylogenetic comparison between Type IX Secretion**
2 **System (T9SS) protein components suggests**
3 **evidence of horizontal gene transfers**

4
5

6 Reeki Emrizal¹, Nor Azlan Nor Muhammad¹

7
8

9 ¹ Centre for Bioinformatics Research, Institute of Systems Biology (INBIOSIS), Universiti
10 Kebangsaan Malaysia, 43600 UKM Bangi, Selangor Darul Ehsan, Malaysia

11

12 Corresponding Author:

13 Nor Azlan Nor Muhammad¹

14 Centre for Bioinformatics Research, Institute of Systems Biology (INBIOSIS), Universiti
15 Kebangsaan Malaysia, 43600 UKM Bangi, Selangor Darul Ehsan, Malaysia

16 Email address: norazlanm@ukm.edu.my

17
18

19
20

21
22

23
24

25
26

27
28

29
30

31
32

33
34

35
36

37 Abstract

38

39 *Porphyromonas gingivalis* is one of the major bacteria that causes periodontitis. Chronic
40 periodontitis is a severe form of periodontal disease that ultimately lead to tooth loss. Virulence
41 factors that contribute to periodontitis are secreted by Type IX Secretion System (T9SS). There
42 are aspects of T9SS protein components that have yet to be characterised. Thus, the aim of this
43 study is to investigate phylogenetic relationship between members of 20 T9SS component
44 protein families. The Bayesian Inference (BI) trees for 19 T9SS protein components exhibit
45 monophyletic clades for all major classes under Bacteroidetes with a strong support for the
46 monophyletic clades or its subclades that is consistent with phylogeny exhibited by the
47 constructed BI tree of 16S rRNA. The BI tree of PorR is different from the 19 BI trees of T9SS
48 protein components as it does not exhibit monophyletic clades for all major classes under
49 Bacteroidetes. There is a strong support for the phylogeny exhibited by BI tree of PorR deviates
50 from the phylogeny based on 16S rRNA. Hence, it is possible that *porR* gene is subjected to
51 horizontal transfer as it is known that virulence factor gene could be horizontally transferred.
52 Seven genes (*porR* included) that involved in the biosynthesis of A-LPS are found to be flanked
53 by insertion sequences (IS5 family transposons). Therefore, the intervening DNA segment that
54 contains *porR* gene might be transposed and subjected to conjugative transfer. Thus, the seven
55 genes can be co-transferred via horizontal gene transfer. The BI tree of UgdA does not exhibit
56 monophyletic clades for all major classes under Bacteroidetes which is similar to the BI tree of
57 PorR (both are a part of the seven genes). Both BI trees also exhibit similar topology as the four
58 identified clusters with a strong support have similar relative positions to each other in both BI
59 trees. This reinforces the possibility that *porR* and the other six genes might be horizontally
60 transferred. Other than the BI tree of PorR, the other 19 BI trees of T9SS protein components
61 also exhibit evidence of horizontal gene transfer. However their genes might undergo horizontal
62 gene transfer less frequently compared to *porR* because the intervening DNA segment that
63 contains *porR* is easily exchanged between bacteria under Bacteroidetes due to the presence of
64 insertion sequences (IS5 family transposons) that flanking it. In conclusion, this study can
65 provide a better understanding about the phylogeny of T9SS protein components.

66

67

68

69

70

71

72

73

74

75

76 Introduction

77

78 Periodontitis is a form of periodontal disease that is driven by the inflammatory conditions that
79 have deteriorating effects on the structures that support the teeth that include gingiva (gum),
80 alveolar bone, and periodontal ligament. Prolonged inflammatory conditions in chronic
81 periodontitis can cause the destruction of those supporting structures that ultimately lead to tooth
82 loss and might contribute to the systemic inflammation (Kinane, Stathopoulou & Papapanou,
83 2017; Escobar et al., 2018). This is evidenced by its implications in systemic diseases such as
84 atherosclerosis (Gotsman et al., 2007), aspiration pneumonia (Benedyk et al., 2016), cancer (Gao
85 et al., 2016), rheumatoid arthritis (Laugisch et al., 2016), and diabetes mellitus (Khader et al.,
86 2006). *Porphyromonas gingivalis* is an oral pathogen that is frequently associated with
87 periodontitis and it is found to acquire Type IX Secretion System (T9SS); a bacterial secretion
88 system that is unique to gram-negative bacteria under Bacteroidetes phylum (Sato et al., 2010).

89 T9SS exhibits diverse roles among species of bacteria under Bacteroidetes. Other than
90 transporting virulence factors such as gingipains and peptidylarginine deiminase in *P. gingivalis*
91 that can cause human oral diseases (Potempa, Pike & Travis, 1995; Maresz et al., 2013), T9SS
92 also transporting virulence factors such as chondroitin sulfate lyases that can cause columnaris
93 disease which is a form of fish disease. *Flavobacterium columnare*, a fish pathogen that
94 contributes to the epidemic that occurred among wild and cultured fishes, is found to acquire
95 T9SS. This epidemic poses a problem to the aquaculture industry as columnaris disease can
96 significantly increase the mortality rate among cultured fishes and thus threatened the industry
97 output (Li et al., 2017). T9SS also involved in the transport of non-virulence factors such as
98 cargo proteins that formed the bacterial gliding motility apparatus in *Flavobacterium johnsoniae*
99 that aids in its motility (Nakane et al., 2013) and enzymes that are importance for lignocellulose
100 digestion in the rumen of ruminants that become the hosts for the *Candidatus*
101 *Paraporphyromonas polyenzymogenes* (Naas et al., 2018).

102 Gram-negative bacteria have an outer membrane (OM) that acts as an impermeable layer
103 that prevents the free movement of hydrophilic and hydrophobic molecules across it. This is
104 because of the presence of lipopolysaccharides (LPS) within the outer leaflet of OM. Outer
105 membrane protein that is embedded in the OM usually forms a channel to allow small molecules
106 to pass through it (Nikaido, 2003; Hong et al., 2006). However, large molecules such as proteins
107 require larger channel to pass through the OM. Hence, secretion systems are developed by
108 bacteria to enable coordinated transport of specific cargo proteins across the OM. Currently,
109 there are nine different types of secretion system evolved by bacteria. T9SS is restricted to
110 bacteria under Bacteroidetes (Sato et al., 2010; Lasica et al., 2017).

111 T9SS is consisted of many different protein components that perform coordinated roles to
112 ensure proper translocation and modification of its cargo proteins. These roles can be categorised
113 into four major functions: translocation, modification, energetic, and regulation (Sato et al.,
114 2010; Lasica et al., 2017; Naito et al., 2019). Initially, the cargo proteins of T9SS are
115 translocated across the inner membrane (IM) via Sec translocon where the signal peptide (SP) of

116 cargo proteins is cleaved (Rahman et al., 2003). The cargo proteins also acquired C-terminal
117 domain (CTD) that interacts with the PorK₂L₃M₂N₂ trans-envelope complex to translocate cargo
118 proteins across periplasm (Vincent et al., 2017; Vincent, Chabaliere & Cascales, 2018) (Fig. 1).
119 PorE has been suggested to form the scaffold of periplasm complex that translocates cargo
120 proteins across the periplasm (Heath et al., 2016; Naito et al., 2019). SprA (ortholog of Sov in *F.*
121 *johnsoniae*) has been proposed as the secretion pore that translocates cargo proteins across OM
122 (Lauber et al., 2018). PorV acts as an outer membrane shuttle protein that delivers the cargo
123 proteins to the attachment complex (Glew et al., 2017) (Fig. 1). In the attachment complex, PorU
124 cleaves the CTD of cargo protein. Then, it is glycosylated with anionic lipopolysaccharide (A-
125 LPS) delivered by PorZ at the cleaved site (Glew et al., 2012, 2017). After both post-
126 translational modifications, the cargo protein will be anchored to cell surface by A-LPS (Lasica
127 et al., 2016; Glew et al., 2017) (Fig. 1). PorX and PorY formed a two-component system (TCS)
128 that regulates the operon of *por* genes (*porP*, *porK*, *porL*, *porM*, and *porN*) via SigP (Vincent et
129 al., 2017; Kadowaki et al., 2016) (Fig. 1). PorR is an aminotransferase that involves in the Wbp
130 pathway that biosynthesis the structural repeating unit of anionic polysaccharide (APS) (Shoji et
131 al., 2002; Shoji et al., 2014) (Fig. 1). Despite that, there are T9SS components without known
132 functions (PorP, PorT, PorW, Omp17, PorF, and PorG) (Fig. 1) and a few aspects of T9SS
133 components that have yet to be characterised (Nguyen et al., 2009; Saiki & Konishi, 2010; Sato
134 et al., 2010; Gorasia et al., 2016; Naito et al., 2019; Taguchi et al., 2016).

135 This work aims to characterise the phylogeny of T9SS protein components. Phylogenetic
136 analysis was performed on the members of 20 T9SS component protein families that have been
137 reported (Emrizal & Muhammad, 2018). The Bayesian Inference (BI) trees for 19 T9SS protein
138 components exhibit monophyletic clades for all major classes under Bacteroidetes with a strong
139 support for the monophyletic clades or its subclades that is consistent with phylogeny exhibited
140 by the constructed BI tree of 16S rRNA. The BI tree of PorR is different from the other 19 BI
141 trees as it does not exhibit monophyletic clades for all major classes under Bacteroidetes. There
142 is also a strong support for the phylogeny exhibited by BI tree of PorR. Thus, there is a
143 possibility that *porR* gene is subjected to horizontal transfer as it is known that virulence factor
144 gene could be horizontally transferred (Hirt, Schlievert & Dunny, 2002). Seven genes including
145 *porR* that involved in the biosynthesis of A-LPS are found to be flanked by insertion sequences
146 (IS5 family transposons). This suggests that the intervening DNA segment that contains *porR*
147 can be transposed and subjected to conjugative transfer (Thomas & Nielsen, 2005; Brochet et al.,
148 2009). Thus, the seven genes might be co-transferred via horizontal gene transfer. The BI trees of
149 PorR and UgdA (both are a part of the seven genes) exhibit similarities. This reinforces the
150 possibility that *porR* and the other six genes might undergo horizontal gene transfer. Other than
151 the BI tree of PorR, the BI trees of other 19 components also exhibit evidence of horizontal gene
152 transfer. However, for the genes that encode those 19 components, they might undergo
153 horizontal gene transfer less frequently compared to *porR* because the intervening DNA segment
154 that contains *porR* is easily exchanged between bacteria under Bacteroidetes due to the presence
155 of IS5 family transposons that flanking it.

156 **Materials & Methods**

157

158 **Construction of multiple sequence alignments of T9SS protein components**

159 The multiple sequence alignments for each T9SS protein component were built using the
160 putative members of T9SS component protein families. The pipeline that was used to select
161 those members has been reported (Emrizal & Muhammad, 2018). The pipeline was used to filter
162 out false positives among the homologs that have been identified through homology searching
163 using BLASTP which was performed using T9SS component protein sequences retrieved from
164 NCBI protein database that were searched against a local BLAST database constructed from
165 completely sequenced bacterial proteomes from Genbank. The selection criteria used in the
166 pipeline: $e\text{-value} \leq 0.001$, query coverage $> 60\%$, and Bacteroidetes homolog with the lowest $e\text{-}$
167 value for bacterial strains with multiple hits; can minimise the possibility of false positives
168 inclusion (Emrizal & Muhammad, 2018). The sequences of protein homologs used to build the
169 multiple sequence alignments for each T9SS component were provided in FASTA format as a
170 Supplemental Information (Data S1).

171 The multiple sequence alignments were constructed using MAFFT version (7.402)
172 (Kato et al., 2002) on the CIPRES computing cluster (Miller, Pfeiffer & Schwartz, 2010). The
173 constructed multiple sequence alignments are in FASTA format. Unreliable alignment regions in
174 the multiple sequence alignments were assessed using Guidance 2 version (2.02) (Sela et al.,
175 2015) on the CIPRES computing cluster (Miller, Pfeiffer & Schwartz, 2010). Columns with low
176 confidence were removed from the multiple sequence alignments. The format of multiple
177 sequence alignments was converted into relaxed interleaved PHYLIP format using online Format
178 Converter (https://www.hiv.lanl.gov/content/sequence/FORMAT_CONVERSION/form.html).
179 The multiple sequence alignments in relaxed interleaved PHYLIP format were manually edited
180 into NEXUS format.

181

182 **Determination of amino acid substitution models for multiple sequence alignments of T9SS** 183 **protein components**

184 The multiple sequence alignments in relaxed interleaved PHYLIP format (Data S2) were used by
185 ProtTest version (3.4.2) (Guindon & Gascuel, 2003; Darriba et al., 2011) to determine amino
186 acid substitution model to be used for each alignment in the phylogenetic analysis. Graphical
187 user interface (GUI) version of ProtTest was used to test each alignment against 10 amino acid
188 substitution model matrices (Blosom62, CpREV, Dayhoff, JTT, MtMam, MtREV, RtREV, VT,
189 WAG, and LG) with any combination of among-site rate variation (no rate variation across sites,
190 gamma-shaped rate variation across sites (+G), a proportion of invariable sites (+I), or gamma-
191 shaped rate variation across sites with a proportion of invariable sites (+G+I)) and stationary
192 amino acid frequencies (Dirichlet or fixed (empirical) (+F)). The best model according to
193 Bayesian Information Criterion (BIC) (Schwarz, 1978) was selected to be used in the
194 phylogenetic analysis for that alignment.

195

196 **Bayesian Inference (BI) analysis for multiple sequence alignments of T9SS protein**
197 **components**

198 Bayesian Inference (BI) analysis was performed using multiple sequence alignments in NEXUS
199 format (Data S3). The BI analysis was performed using MrBayes version (3.2.6) (Huelsenbeck &
200 Ronquist, 2001) on the CIPRES computing cluster (Miller, Pfeiffer & Schwartz, 2010) for
201 alignments of 14 components (PorK, PorL, PorM, PorN, PorP, PorQ, PorT, PorU, PorV, SigP,
202 Omp17, PorE, PorF, and PorG). The BI analysis for each alignment was performed with the
203 selected amino acid substitution model and two independent runs, for 50,000,000 generations,
204 each with four chains, with a sampling frequency of every 5,000, and a burn-in of 25%. Beagle
205 CPU was utilised to speed up the BI analysis.

206 The BI analysis for the other 6 components (PorR, Sov, PorW, PorX, PorY, and PorZ)
207 was performed using command-line MrBayes version (3.2.6) (Huelsenbeck & Ronquist, 2001)
208 on a desktop with Nvidia Titan V GPU and CUDA driver version (10.1) installed. The BI
209 analysis for each alignment was performed with the selected amino acid substitution model and
210 two independent runs, for 50,000,000 generations, each with four chains (PorR, Sov, PorW) or
211 eight chains (PorX, PorY, and PorZ), with a sampling frequency of every 5,000, and a burn-in of
212 25%. Beagle GPU was utilised to speed up the BI analysis. The constructed BI trees were
213 visualised and annotated using online iTOL version (4.4.2) (Letunic & Bork, 2019).

214

215 **Construction of Bayesian Inference (BI) tree of 16S ribosomal RNA (rRNA)**

216 The 16S ribosomal RNA (rRNA) sequences have been used to construct the current universal
217 tree of life (Winker & Woese, 1991; Pylro et al., 2012). Thus, the BI tree of 16S rRNA has been
218 constructed in this work to compare it with the BI trees of T9SS protein components. A pre-
219 formatted BLAST database of microbial 16S rRNA sequences was retrieved from NCBI
220 (<ftp://ftp.ncbi.nlm.nih.gov/blast/db/>). The 16S rRNA sequence from *Porphyromonas gingivalis*
221 ATCC 33277 (NR_040838.1) was retrieved from NCBI (<https://www.ncbi.nlm.nih.gov/gene>)
222 and it was searched against that database using local BLASTN (Altschul et al., 1990). The
223 pipeline mentioned above was used to select homologs of 16S rRNA gene in species under
224 Bacteroidetes that are also found to acquire homologs of T9SS protein components in this work.
225 For those species that their 16S rRNA sequences could not be retrieved from the microbial 16S
226 rRNA BLAST database, their 16S rRNA sequences were retrieved directly from either the NCBI
227 Gene (<https://www.ncbi.nlm.nih.gov/gene>) or NCBI Nucleotide (<https://www.ncbi.nlm.nih.gov/nucleotide>). The selected 16S rRNA sequences were provided in FASTA format as a Supplemental
228 Information (Data S1).
229

230 The sequences were used to build the multiple sequence alignment of 16S rRNA using
231 MAFFT version (7.402) (Katoh et al., 2002) and unreliable alignment regions in the multiple
232 sequence alignment were assessed using Guidance 2 version (2.02) (Sela et al., 2015) on the
233 CIPRES computing cluster (Miller, Pfeiffer & Schwartz, 2010). Columns with low confidence
234 were removed from the multiple sequence alignment. The alignment in FASTA format (Data S2)
235 was used to determine the best nucleotide substitution model to be used in the phylogenetic

236 analysis. Graphical user interface (GUI) version of ModelTest (Darriba et al., 2019) was used to
237 test the alignment against 3 nucleotide substitution model matrices (GTR, HKY85, and F81)
238 with any combination of among-site rate variation (no rate variation across sites, gamma-shaped
239 rate variation across sites (+G), a proportion of invariable sites (+I), or gamma-shaped rate
240 variation across sites with a proportion of invariable sites (+G+I)) and stationary amino acid
241 frequencies (Dirichlet or fixed (empirical) (+F)). The best model according to Bayesian
242 Information Criterion (BIC) (Schwarz, 1978) was selected to be used in the phylogenetic
243 analysis for that alignment.

244 BI analysis was performed using the alignment in NEXUS format (Data S3). The analysis
245 was performed using MrBayes version (3.2.6) (Huelsenbeck & Ronquist, 2001) on the CIPRES
246 computing cluster (Miller, Pfeiffer & Schwartz, 2010) with the selected nucleotide substitution
247 model and two independent runs, for 50,000,000 generations, each with four chains, with a
248 sampling frequency of every 5,000, and a burn-in of 25%. Beagle CPU was utilised to speed up
249 the BI analysis. The BI tree of 16S rRNA was visualised and annotated using online iTOL
250 version (4.4.2) (Letunic & Bork, 2019).

251

252 **Identification of *porR* and its neighbouring genes arrangement in *Porphyromonas gingivalis*** 253 **ATCC 33277 genome**

254 The sequence of *P. gingivalis* ATCC 33277 genome and annotation files of the genome were
255 retrieved from Genbank (Naito et al., 2008). The *P. gingivalis* ATCC 33277 genome sequence
256 and its annotation files were provided in the Supplemental Information (Data S4). The part of *P.*
257 *gingivalis* ATCC 33277 genome sequence that contains the *porR* and its neighbouring genes was
258 extracted. Then, it was searched against the non-redundant protein sequences (nr) database using
259 online BLASTX. The search was narrowed down to the proteome of *P. gingivalis* ATCC 33277
260 only. The maximum target sequences were set at highest value available which is 20,000. Other
261 parameters were left at its default values (Altschul et al., 1990). Only the matches with 100%
262 percentage identity and 0 e-value were used to annotate the part of *P. gingivalis* ATCC 33277
263 genome sequence that contains *porR* gene.

264

265 **Construction of Bayesian Inference (BI) tree of UgdA**

266 Based on identification of *porR* neighbouring genes, the two genes that involve in Wbp pathway
267 (*ugdA* and *porR*) are found to be within the intervening DNA segment that is flanked by IS5
268 family transposons. Thus, BI tree of UgdA was constructed to be compared with BI tree of PorR.
269 The pipeline mentioned above was used to select homologs of UgdA (Data S1) and construct the
270 multiple sequence alignment of UgdA with low confidence columns being removed. The
271 alignment in relaxed interleaved PHYLIP format (Data S2) was used to determine the best amino
272 acid substitution model. BI analysis was performed using UgdA alignment in NEXUS format
273 (Data S3). The analysis was performed using command-line MrBayes version (3.2.6)
274 (Huelsenbeck & Ronquist, 2001) on a desktop with Nvidia Titan V GPU and CUDA driver
275 version (10.1) installed with the selected amino acid substitution model and two independent

276 runs, for 50,000,000 generations, each with four chains, with a sampling frequency of every
277 5,000, and a burn-in of 25%. Beagle GPU was utilised to speed up the BI analysis. The
278 constructed BI tree was visualised and annotated using online iTOL version (4.4.2) (Letunic &
279 Bork, 2019).

280

281 **Results**

282

283 **Bayesian Inference (BI) trees of T9SS protein components**

284 Bayesian Inference (BI) trees are constructed from the multiple sequence alignments of putative
285 members of T9SS component protein families that have been reported (Emrizal & Muhammad,
286 2018). The characteristics of alignments and the best amino acid substitution model that has been
287 selected for each alignment are shown in Table 1. The selected amino acid substitution model for
288 each alignment defines the parameters that are used for BI analysis for each alignment. The
289 unrooted BI trees of T9SS protein components are shown (Figs. 2-6). The identified
290 monophyletic clades that formed by terminal nodes that belong to the same class under
291 Bacteroidetes are denoted by solid curves (Figs. 2-6). The monophyletic clades or its subclades
292 with a strong support (posterior probability value > 0.95) are denoted by dashed curves (Figs. 2-
293 6).

294 Out of 20 BI trees of T9SS protein components, only 19 exhibit monophyletic clades for
295 all major classes under Bacteroidetes (Figs. 2-6). Major classes are those with more than five
296 families under the classes (Bacteroidia, Cytophagia, and Flavobacteriia) while minor classes are
297 those with less than or equal to five families under the classes (Chitinophagia, Sphingobacteriia,
298 Saprospiria, Incertae sedis, and unclassified). Nine of the BI trees (PorK, Sov, PorT, PorV,
299 PorW, PorX, Omp17, PorE, and PorF) exhibit monophyletic clades for all major classes under
300 Bacteroidetes with a strong support. Ten of the BI trees (PorL, PorM, PorN, PorP, PorQ, PorU,
301 PorY, PorZ, SigP, and PorG) exhibit strong support for the monophyletic clades or its subclades
302 for all major classes under Bacteroidetes (Figs. 2-6). Despite the presence of PorR homologs
303 from species under Bacteroidia, Cytophagia, and Flavobacteriia, the BI tree of PorR does not
304 exhibit monophyletic clades for all major classes under Bacteroidetes (Fig. 3C). Thus, the BI tree
305 of PorR is different compared to the other 19 BI trees of T9SS protein components that exhibit
306 monophyletic clades for all major classes under Bacteroidetes.

307 Some of the terminal nodes of 19 BI trees of T9SS protein components are out of its
308 expected monophyletic clades (Figs. 2-6). The species corresponding to those terminal nodes are
309 listed in Table S1. There are species that frequently have their terminal nodes out of its expected
310 monophyletic clades such as *Fluviicola taffensis* DSM 16823, bacterium L21-Spi-D4,
311 *Owenweeksia hongkongensis* DSM 17368, and *Draconibacterium orientale*. The terminal nodes
312 corresponding to *F. taffensis* DSM 16823 are found to be out of its expected monophyletic clades
313 in 14 out of 19 BI trees (except PorK, PorN, PorP, PorU, and SigP). The terminal nodes
314 corresponding to bacterium L21-Spi-D4 are found to be out of its monophyletic clades in 10 out
315 of 19 BI trees (except PorK, PorL, PorM, Sov, PorT, PorU, PorX, PorY, and PorE). The terminal

316 nodes corresponding to *O. hongkongensis* DSM 17368 are found to be out of its expected
317 monophyletic clades in 6 out of 19 BI trees (PorM, PorP, PorV, PorY, Omp17, and PorE). The
318 terminal nodes corresponding to *D. orientale* are found to be out of its expected monophyletic
319 clades in 7 out of 19 BI trees (PorN, PorP, PorV, PorW, PorY, SigP, and Omp 17). The 20 BI
320 trees with terminal nodes labelled with its corresponding species and support values for each
321 branch are shown are provided in the Supplemental Information (Figs. S1-S20).

322

323 **Bayesian Inference (BI) tree of 16S rRNA**

324 The BI tree of 16S rRNA is constructed from the multiple sequence alignment of 16S rRNA
325 homologs from species that are identified to also acquire T9SS protein homologs. Out of 181
326 species that acquire T9SS protein homologs, only 16S rRNA sequences from 144 species are
327 able to be retrieved from NCBI. The characteristic of 16S rRNA alignment and the best
328 nucleotide substitution model that has been selected for that alignment are shown in Table 1. The
329 unrooted BI tree of 16S rRNA is shown in Fig. 7. The identified monophyletic clades that
330 formed by terminal nodes that belong to the same class under Bacteroidetes are denoted by solid
331 curves (Fig. 7). The monophyletic clades or its subclades with a strong support (posterior
332 probability value > 0.95) are denoted by dashed curves (Fig. 7).

333 The BI tree of 16S rRNA is constructed to be compared to the BI trees of T9SS protein
334 components. The 16S rRNA exhibits monophyletic clades for all major classes under
335 Bacteroidetes with a strong support (Fig. 7) similar to the 19 BI trees of T9SS protein
336 components. The 16S rRNA also exhibits monophyletic clades for all minor classes under
337 Bacteroidetes with a strong support denoted by 4 monophyletic clades of red, pink, yellow and
338 orange circles (Fig. 7). None of the 20 BI trees of T9SS protein components exhibit phylogeny of
339 the minor classes that is consistent to the phylogeny exhibits by the 16S rRNA tree (Fig. 2-7).
340 Hence, minor classes are excluded in the comparison between 20 BI trees of T9SS protein
341 components. The BI tree of 16S rRNA with terminal nodes labelled with its corresponding
342 species and support values for each branch are shown is provided in the Supplemental
343 Information (Fig. S21).

344

345 **Arrangement of *porR* and its neighbouring genes in *P. gingivalis* ATCC 33277 genome**

346 As shown in Fig. 8, *porR* and its neighbouring genes are flanked by IS5 family transposons. The
347 IS5 family transposon (cyan rectangles) encodes IS5 family transposase that cleaves the flanking
348 12 bp inverted repeats (purple triangles) (Fig. 8). This might suggest the possibility that
349 intervening DNA segment that contains seven genes that involved in A-LPS biosynthesis (yellow
350 rectangles) can undergo transposition and possibly subjected to conjugative transfer (Fig. 8)
351 (Thomas & Nielsen, 2005; Brochet et al., 2009). *porR* (PGN_1236) and *ugdA* (PGN_1243)
352 genes (Fig. 8) have been reported to be involved in Wbp pathway that is important for the
353 biosynthesis of structural sugar (di-acetylated glucuronic acid) of A-LPS (Shoji et al., 2002;
354 Shoji et al., 2014). *porS* (PGN_1235) and *wzy* (PGN_1242) genes (Fig. 8) have been reported to
355 participate in the assembly of A-LPS in bacterial inner membrane (Shoji et al., 2013). *gtfB*

356 (PGN_1251) and *gtfE* (PGN_1240) glycosyltransferases genes (Fig. 8) are important for A-LPS
357 biosynthesis while *rfa* (PGN_1255) glycosyltransferase gene (Fig. 8) is important for
358 biosynthesis of lipid A-core portion of A-LPS (Shoji et al., 2018).

359

360 **Bayesian Inference (BI) tree of UgdA**

361 The BI tree of UgdA is constructed from the multiple sequence alignment of UgdA homologs
362 that are identified using the same pipeline that has been reported to select T9SS protein
363 homologs (Emrizal & Muhammad, 2018). The characteristic of UgdA alignment and the best
364 amino acid substitution model that has been selected for that alignment are shown in Table 1.
365 The unrooted BI tree of UgdA is shown in Fig. 9B. The unrooted BI tree of PorR is also shown
366 in Fig. 9A to be compared with the BI tree of UgdA. Both BI trees do not exhibit monophyletic
367 clades for all major classes under Bacteroidetes. Both BI trees also exhibit similar topology. Four
368 similar clusters (I, II, III, and IV) have been identified between both BI trees. Cluster I consists
369 primarily of terminal nodes from Flavobacteriia and a few terminal nodes from other classes.
370 Cluster II consists of terminal nodes from Porphyromonas, Tannerella, and Parabacteroides
371 genera. Cluster III consists of terminal nodes from Rufibacter and Hymenobacter genera. Cluster
372 IV consists of terminal nodes from Prevotella, Bacteroides, Proteiniphilum and other genera. The
373 BI tree of UgdA with terminal nodes labelled with its corresponding species and support values
374 for each branch are shown is provided in the Supplemental Information (Fig. S22).

375

376 **Taxonomic distribution of T9SS protein components**

377 As shown in the 20 BI trees of T9SS components (Figs. 2-6), only bacteria under Bacteroidia,
378 Flavobacteriia, and Chitinophagia classes acquired the 20 components investigated in this work.
379 The bacteria under Cytophagia class acquired only 19 protein components (except PorN). The
380 bacteria under Saprospiria class acquired only 18 protein components (except PorL and PorG).
381 The bacteria under Sphingobacteriia class acquired only 17 protein components (except PorQ,
382 PorU, and PorZ). The bacteria under unclassified acquired only 17 protein components (except
383 PorN, PorU, and PorG). The bacteria under Incertae sedis class acquired only 11 protein
384 components (PorQ, PorR, Sov, PorU, PorV, PorX, PorY, PorZ, SigP, Omp17, and PorF).

385 The finding in this work is consistent with the taxonomic distribution of T9SS
386 components among bacteria under Bacteroidetes where it has been reported that Bacteroidia,
387 Flavobacteriia, Cytophagia, Sphingobacteriia, and Incertae sedis classes acquired T9SS
388 component homologs (McBride & Zhu, 2013). However, comparing the reported taxonomic
389 distribution of T9SS components to the finding in this work, we have identified other species
390 under Chitinophagia, Saprospiria, and unclassified that acquired T9SS component homologs.
391 Those species and T9SS component homologs they acquired are illustrated in Fig. 10.

392

393

394

395 **Discussion**

396

397 The 19 Bayesian Inference (BI) trees of T9SS protein components exhibit monophyletic clades
398 for all major classes under Bacteroidetes with a strong support for the monophyletic clades or its
399 subclades (Figs. 2-6). Similar to the 19 BI trees of T9SS protein components, the BI tree of 16S
400 rRNA also exhibits monophyletic clades for all major classes under Bacteroidetes with a strong
401 support (Fig. 7). 16S rRNA has been extensively used in phylogenetic analysis for the purpose of
402 evolutionary comparison and classification. The reliability of this approach lies on the
403 assumption that 16S rRNA gene undergoes hierarchical and unidirectional evolution and no gene
404 transfer of 16S rRNA occurs between species (Karlsson et al. 2011). Due to the advantages that
405 16S rRNA gene has such as ubiquitous gene in bacterial genomes, easily sequenced, and widely
406 available in public sequence databases, the current universal tree of life is based on the
407 phylogeny of this gene (Winker & Woese, 1991; Coutinho et al., 1999; Pylro et al., 2012). That
408 assumption has been challenged due to the presence of multiple copies of 16S rRNA in a
409 bacterial genome and the 16S rRNA genes from operons in the same genome are rather distinct
410 which might suggest such gene might have undergo horizontal gene transfer (Pei et al., 2010;
411 Karlsson et al., 2011). However, the extent of 16S rRNA evolution remains considerably less
412 compared to the other genes in the bacterial genome (Espejo & Plaza, 2018). Thus, 16S rRNA
413 remains relevant for the purpose of evolutionary comparison and classification.

414 It is expected that the BI trees of T9SS protein components would exhibit similar
415 phylogeny with the BI tree of 16S rRNA. However, the BI trees of T9SS protein components
416 exhibit inconsistent positions of terminal nodes from minor classes among themselves and the
417 phylogeny for the minor classes that deviates from the phylogeny exhibited by BI tree of 16S
418 rRNA (Figs. 2-7). Hence, the minor classes under Bacteroidetes are excluded in the comparison
419 between the 20 BI trees of T9SS protein components. This might arise due to insufficient taxa
420 from minor classes provided to construct those BI trees. Hence, less information is provided
421 which is insufficient to fully resolve the phylogeny of minor classes. As more T9SS-acquiring
422 species from minor classes are sequenced later on, probably the phylogeny of T9SS protein
423 components will be more resolved (Alvizu et al., 2018).

424 Different from the other 19 BI trees of T9SS protein components, the BI tree of PorR
425 does not exhibit monophyletic clades for all major classes under Bacteroidetes (Figs. 2-6).
426 The presence of a strong support (posterior probability value > 0.95) as denoted by the black
427 branch leading to the top half of BI tree of PorR (Fig. 3C) suggests that there is a strong support
428 for the phylogeny exhibited by BI tree of PorR deviates from the phylogeny based on 16S rRNA
429 sequence (Fig. 7). Thus, there is a possibility that *porR* gene is subjected to horizontal transfer
430 hence causing deviation from the expected phylogeny (Pylro et al., 2012). Hirt, Schlievert &
431 Dunny have demonstrated that virulence factor and antibiotic resistance genes could be
432 horizontally transferred (Hirt, Schlievert & Dunny, 2002). Hence, this suggests the possibility
433 that *porR* gene that encodes one of the virulence factors produced by *P. gingivalis* can be
434 horizontally transferred (Shoji et al., 2002; Shoji et al., 2014).

435 The arrangement of *porR* and its neighbouring genes in the *P. gingivalis* ATCC 33277
436 genome is identified in order to support the possibility that *porR* is horizontally transferred. *P.*
437 *gingivalis* ATCC 33277 genome is chosen because many gene orthologs that involved in A-LPS
438 biosynthesis have been identified in this genome (Shoji et al., 2018). *porR* and its neighbouring
439 genes are found to be flanked by insertion sequences (IS5 family transposons) (Fig. 8). The IS5
440 family transposons (cyan rectangles) contain a single open reading frame that encodes for IS5
441 family transposase that cleaves the 12 bp inverted repeats (purple triangles) that flanked the
442 insertion sequences (Fig. 8). The 12 bp inverted repeats show imperfect homology to each other
443 with the consensus sequence: GAGACCTTTG[CA]A. Both of the IS5 family transposons are
444 ~1300 bp in length. These features are typical of IS5 family transposons (Mahillon & Chandler,
445 1998; Naito et al., 2008). The intervening DNA segment and both IS5 family transposons that
446 flanked it might form a composite transposon where the cleaving action of IS5 family
447 transposases on inverted repeats can mobilise the intervening DNA segment that contains *porR*
448 gene and possibly subjected it to conjugative transfer (Thomas & Nielsen, 2005; Brochet et al.,
449 2009). The length of the composite transposon is ~70 kbp. However, it is also possible for IS5
450 family transposase to cleave the inverted repeat directly downstream of *rfa* (PGN_1255) (Fig. 8)
451 which will reduce the length of composite transposon to ~47 kbp. It has been reported that a
452 transposon of ~47 kbp in length is able to undergo both transposition and conjugation processes
453 (Brochet et al., 2009). Hence, it might be possible for composite transposon of such length to
454 undergo transposition and subsequently being horizontally transferred via bacterial conjugation.

455 The intervening DNA segment contains seven genes that involved in the biosynthesis of
456 A-LPS (Fig. 8). Both *porR* (PGN_1236) and *ugdA* (PGN_1243) genes are involved in Wbp
457 pathway that is important for biosynthesis of di-acetylated glucuronic acid that is the structural
458 sugar of A-LPS (Shoji et al., 2002; Shoji et al., 2014). The *porS* gene (PGN_1235), which is an
459 O-antigen flippase, and *wzy* gene (PGN_1242), which is an O-antigen polymerase, are involved
460 in the assembly of A-LPS at the periplasmic side of bacterial IM (Shoji et al., 2013). *gtfB*
461 (PGN_1251) and *gtfE* (PGN_1240) glycosyltransferases genes are involved in the biosynthesis
462 of sugar moiety of A-LPS. *rfa* (PGN_1255) glycosyltransferase gene is involved in the
463 biosynthesis of lipid A-core moiety of A-LPS (Shoji et al., 2018). However, there are other genes
464 that involved in the biosynthesis of A-LPS and they are spread out throughout the genome (Shoji
465 et al., 2018). Usually, genes that are co-regulated and involved in a similar pathway are clustered
466 in a single operon (Yanofsky & Lennox, 1959; Osbourn & Field, 2009). Thus, it is possible that
467 the other genes do not form a cluster with the seven genes that are identified to be flanked by
468 insertion sequences (IS5 family transposons) because they are not co-regulated.

469 It is possible that those seven genes might be co-transferred via horizontal gene transfer.
470 Thus, phylogenetic analysis is performed for the protein alignment of UgdA that is encoded by
471 *ugdA* that, together with *porR*, are involved in the Wbp pathway and are co-localised in the
472 intervening DNA segment flanked by IS5 family transposons (Fig. 8). The BI tree of UgdA (Fig.
473 9B) is constructed to be compared with the BI tree of PorR (Fig. 9A). Different to the 19 BI trees
474 of T9SS protein components, both BI trees do not exhibit monophyletic clades for all major

475 classes under Bacteroidetes. They also exhibit similar topology where four similar clusters (I, II,
476 III, and IV) with a strong support (denoted by a black branch leading to the cluster) have been
477 identified in both BI trees. Cluster I consists of terminal nodes from Flavobacteriia and a few
478 terminal nodes from other classes. Cluster II consists of terminal nodes from Porphyromonas,
479 Tannerella, and Parabacteroides genera. Cluster III consists of terminal nodes from Rufibacter
480 and Hymenobacter genera. Cluster IV consists of terminal nodes from Prevotella, Bacteroides,
481 Proteiniphilum and other genera. These four clusters exhibit similar relative positions to each
482 other in both BI trees (e.g. cluster I is closer to cluster II than the other clusters and cluster III is
483 closer to cluster II than the other clusters). However, due to the differences in branch lengths
484 between both BI trees, they look slightly different as the upper part of UgdA tree (Fig. 9B)
485 appears more elongated than the upper part of PorR tree (Fig. 9A) while the lower part of UgdA
486 tree (cluster I) appears more shorten than the lower part of PorR tree (cluster I).

487 Other than the BI tree of PorR, the BI trees of other 19 T9SS protein components also
488 exhibit evidence of horizontal gene transfer perhaps between classes under Bacteroidetes. As
489 listed in Table S1, there are terminal nodes that are out of its expected monophyletic clades in the
490 BI trees of those components that suggest the genes that encode them might be horizontally
491 transferred. In theory, the common ancestral species of a monophyletic clade for a class under
492 Bacteroidetes passes the gene that encodes T9SS protein component to its descendant species.
493 Thus, the descendant species that are out of its expected monophyletic clades most likely acquire
494 that gene from the common ancestral species of a monophyletic clade from another class that
495 could be interpreted as a horizontal gene transfer between classes under Bacteroidetes (Thomas
496 & Nielsen, 2005; Brochet et al., 2009). It is interesting to highlight that there are species that
497 frequently have their corresponding terminal nodes in those 19 BI trees out of its expected
498 monophyletic clades (Figs. 2-6) such as *F. taffensis* DSM 16823, bacterium L21-Spi-D4, *O.*
499 *hongkongensis* DSM 17368, and *D. orientale*. Thus, it likely that those bacteria frequently
500 acquire their T9SS components through horizontal gene transfer. However, for the genes that
501 encode those 19 components, they might undergo horizontal gene transfer less frequently
502 compared to *porR* that causes most of the terminal nodes of BI trees of those components are still
503 clustering according to their respective classes. It might be because the intervening DNA
504 segment that contains *porR* gene is easily exchanged between bacteria under Bacteroidetes due
505 to the present of insertion sequences (IS5 family transposons) that flanking it (Fig. 8).

506 T9SS is made up of various protein components that formed the regulation, translocation,
507 energetic, and modification components. Currently, the secretion system is primarily found in
508 bacteria under Bacteroidetes phylum (Abby et al., 2016). Bacteria from classes under
509 Bacteroidetes (Bacteroidia, Flavobacteriia, Cytophagia, Chitinophagia, Sphingobacteriia,
510 Saprospiria, Incertae sedis, and unclassified) are found to acquire T9SS protein components
511 (Figs. 2-6). However, not all of them acquire the 20 components that have been reported (Sato et
512 al., 2010; Lasica et al., 2017). As shown in the 20 BI trees of T9SS protein components (Figs. 2-
513 6), only bacteria under Bacteroidia, Flavobacteriia, and Chitinophagia acquired the 20
514 components investigated. The bacteria under Cytophagia only acquired 19 components (except

515 PorN). The bacteria under Saprospira only acquired 18 components (except PorL and PorG).
516 The bacteria under Sphingobacteriia only acquired 17 components (except PorQ, PorU, and
517 PorZ). The bacteria under unclassified only acquired 17 components (except PorN, PorU, and
518 PorG). The bacteria under Incertae sedis only acquired 11 components (PorQ, PorR, Sov, PorU,
519 PorV, PorX, PorY, PorZ, SigP, Omp17, and PorF). It is interesting to note that PorU, PorZ, and
520 PorQ formed the modification components of T9SS. Thus, Sphingobacteriia does not acquire the
521 components that performed post-translational modifications on T9SS cargo proteins such as
522 cleavage of CTD and A-LPS glycosylation. Perhaps, T9SS acquired by Sphingobacteriia does
523 not cleave the CTD of cargo protein and glycosylate it with A-LPS but leave the cargo protein
524 bounded to PorV after it is translocated to bacterial cell surface by Sov. Other possible
525 explanation is that Sphingobacteriia does have proteins that performed the functions of missing
526 protein components. However, those proteins exhibited limited sequence similarity with any
527 currently known T9SS protein component. Thus, they could not be detected by homology
528 searching method used in this work. This explanation could also be applied for other species of
529 bacteria under Bacteroidetes that do not acquire the homologs of 20 T9SS components.

530 This work has found other species under Chitinophagia, Saprospira, and unclassified that
531 acquired homologs of T9SS components that, to our knowledge, might not have been reported
532 (McBride & Zhu, 2013). Those other species and the homologs of T9SS components they
533 acquired are shown in Fig. 10. This identification might be due to the analysis that has been
534 performed might cover more bacterial species than the previous work as more bacterial genomes
535 have been completely sequenced in the past few years.

536

537 **Conclusions**

538

539 The objective of this work is to investigate the phylogenetic relationship among putative
540 members of 20 T9SS component protein families (Emrizal & Muhammad, 2018). The Bayesian
541 Inference (BI) trees for 19 T9SS protein components exhibit monophyletic clades for all major
542 classes under Bacteroidetes with a strong support for the monophyletic clades or its subclades
543 which is consistent with phylogeny exhibited by the constructed BI tree of 16S rRNA. However,
544 the BI tree of PorR is different from the other 19 BI trees of T9SS protein components as it does
545 not exhibit monophyletic clades for all major classes under Bacteroidetes. There is a strong
546 support for the phylogeny exhibited by BI tree of PorR deviates from the phylogeny based on
547 16S rRNA sequence. Thus, there is a possibility that *porR* gene is subjected to horizontal transfer
548 as it is known that virulence factor gene could be horizontally transferred. Seven genes that
549 involved in the biosynthesis of A-LPS that includes *porR* are found to be flanked by insertion
550 sequences (IS5 family transposons). This suggests that the intervening DNA segment that
551 contains *porR* gene can be transposed and subjected to conjugative transfer. Thus, the seven
552 genes might be co-transferred via horizontal gene transfer. Similar to the BI tree of PorR, the BI
553 tree of UgdA does not exhibit monophyletic clades for all major classes under Bacteroidetes
554 (both are a part of the seven genes). Both BI trees also exhibit similar topology where the four

555 identified clusters with a strong support have similar relative positions to each other in both BI
556 trees. Other than the BI tree of *PorR*, the BI trees of other 19 components also exhibit evidence
557 of horizontal gene transfer. However, for the genes that encode those 19 components, they might
558 undergo horizontal gene transfer less frequently compared to *porR* because the intervening DNA
559 segment that contains *porR* is easily exchanged between bacteria under Bacteroidetes due to the
560 presence of insertion sequences (IS5 family transposons) that flanking it. This work also found
561 other species under Chitinophagia, Saprospira, and unclassified that acquired T9SS component
562 protein homologs that, to our knowledge, might not have been reported.

563

564 Acknowledgements

565

566 The authors acknowledge Universiti Kebangsaan Malaysia (UKM) grant, DPP-2018-010 for
567 providing funds to support this work. We gratefully acknowledge the support of NVIDIA
568 Corporation with the donation of the Titan V GPU used for this research. We thank Centre for
569 Bioinformatics Research (CBR) for providing the facilities to conduct the bioinformatics
570 analyses. We thank the reviewers for their comments on previous drafts of the manuscript.

571

572 References

573

- 574 **Abby SS, Cury J, Guglielmini J, Néron B, Touchon M, Rocha EPC. 2016.** Identification of
575 protein secretion systems in bacterial genomes. *Scientific Reports* **6**:23080 DOI
576 10.1038/srep23080.
- 577 **Altschul SF, Gish W, Miller W, Myers EW, Lipman DJ. 1990.** Basic local alignment search
578 tool. *Journal of Molecular Biology* **215**(3):403–410 DOI 10.1016/S0022-2836(05)80360-2.
- 579 **Alvizu A, Eilertsen MH, Xavier JR, Rapp HT. 2018.** Increased taxon sampling provides new
580 insights into the phylogeny and evolution of the subclass Calcaronea (Porifera, Calcarea).
581 *Organisms Diversity and Evolution* **18**(3):279–290 DOI 10.1007/s13127-018-0368-4.
- 582 **Benedyk M, Mydel PM, Delaleu N, Plaza K, Gawron K, Milewska A, Maresz K, Koziel J,
583 Pyrc K, Potempa J. 2016.** Gingipains: critical factors in the development of aspiration
584 pneumonia caused by *Porphyromonas gingivalis*. *Journal of Innate Immunity* **8**(2):185–198
585 DOI 10.1159/000441724.
- 586 **Brochet M, Da Cunha V, Couvé E, Rusniok C, Trieu-Cuot P, Glaser P. 2009.** Atypical
587 association of DDE transposition with conjugation specifies a new family of mobile
588 elements. *Molecular Microbiology* **71**(4):948–959 DOI 10.1111/j.1365-2958.2008.06579.x.
- 589 **Coutinho HL, De VO, Manfio GP, Rosado AS. 1999.** Evaluating the microbial diversity of soil
590 samples: methodological innovations. *Anais da Academia Brasileira de Ciências* **71**(3 Pt
591 2):491–503
- 592 **Darriba D, Taboada GL, Doallo R, Posada D. 2011.** ProtTest 3: fast selection of best-fit
593 models of protein evolution. *Bioinformatics* **27**(8):1164–1165 DOI
594 10.1093/bioinformatics/btr088.
- 595 **Darriba D, Posada D, Kozlov AM, Stamatakis A, Morel B, Flouri T. 2019.** ModelTest-NG:
596 A New and Scalable Tool for the Selection of DNA and Protein Evolutionary Models.
597 *Molecular Biology and Evolution*:msz189 DOI 10.1093/molbev/msz189.

- 598 **Emrizal R, Muhammad NAN. 2018.** Identification of sequence motifs for the protein
599 components of type IX secretion system. *Sains Malaysiana* **47(12)**:2941–2950 DOI
600 10.17576/jsm-2018-4712-02.
- 601 **Escobar GF, Abdalla DR, Beghini M, Gotti VB, Junior VR, Napimoga MH, Ribeiro BM,**
602 **Rodrigues DBR, Nogueira RD, de Lima Pereira SA. 2018.** Levels of pro and anti-
603 inflammatory cytokines and c-reactive protein in patients with Chronic Periodontitis
604 submitted to nonsurgical periodontal treatment. *Asian Pacific Journal of Cancer*
605 *Prevention : APJCP* **19(7)**:1927–1933 DOI 10.22034/APJCP.2018.19.7.1927.
- 606 **Espejo RT, Plaza N. 2018.** Multiple Ribosomal RNA Operons in Bacteria; Their Concerted
607 Evolution and Potential Consequences on the Rate of Evolution of Their 16S rRNA.
608 *Frontiers in Microbiology* **9**:1232 DOI 10.3389/fmicb.2018.01232.
- 609 **Gao S, Li S, Ma Z, Liang S, Shan T, Zhang M, Zhu X, Zhang P, Liu G, Zhou F, Yuan X,**
610 **Jia R, Potempa J, Scott DA, Lamont RJ, Wang H, Feng X. 2016.** Presence of
611 *Porphyromonas gingivalis* in esophagus and its association with the clinicopathological
612 characteristics and survival in patients with esophageal cancer. *Infectious Agents and*
613 *Cancer* **11(1)**:3 DOI 10.1186/s13027-016-0049-x.
- 614 **Glew MD, Veith PD, Chen D, Gorasia DG, Peng B, Reynolds EC. 2017.** PorV is an outer
615 membrane shuttle protein for the type IX secretion system. *Scientific Reports* **7(1)**:8790
616 DOI 10.1038/s41598-017-09412-w.
- 617 **Glew MD, Veith PD, Peng B, Chen YY, Gorasia DG, Yang Q, Slakeski N, Chen D, Moore**
618 **C, Crawford S, Reynolds EC. 2012.** PG0026 is the C-terminal signal peptidase of a novel
619 secretion system of *Porphyromonas gingivalis*. *Journal of Biological Chemistry*
620 **287(29)**:24605–24617 DOI 10.1074/jbc.M112.369223.
- 621 **Gorasia DG, Veith PD, Hanssen EG, Glew MD, Sato K, Yukitake H, Nakayama K,**
622 **Reynolds EC. 2016.** Structural insights into the PorK and PorN components of the
623 *Porphyromonas gingivalis* type IX secretion system. *PLoS Pathogens* **12(8)**:e1005820 DOI
624 10.1371/journal.ppat.1005820.
- 625 **Gotsman I, Lotan C, Soskolne WA, Rassovsky S, Pugatsch T, Lapidus L, Novikov Y,**
626 **Masrawa S, Stabholz A. 2007.** Periodontal destruction is associated with coronary artery
627 disease and periodontal infection with acute coronary syndrome. *Journal of Periodontology*
628 **78(5)**:849–858 DOI 10.1902/jop.2007.060301.
- 629 **Guindon S, Gascuel O. 2003.** A simple, fast, and accurate algorithm to estimate large
630 phylogenies by maximum likelihood. *Systematic Biology* **52(5)**:696–704 DOI
631 10.1080/10635150390235520.
- 632 **Heath JE, Seers CA, Veith PD, Butler CA, Muhammad NAN, Chen YY, Slakeski N, Peng**
633 **B, Zhang L, Dashper SG, Cross KJ, Cleal SM, Moore C, Reynolds EC. 2016.** PG1058
634 is a novel multidomain protein component of the bacterial type IX secretion system. *PloS*
635 *One* **11(10)**:e0164313 DOI 10.1371/journal.pone.0164313.
- 636 **Hirt H, Schlievert PM, Dunny GM. 2002.** In vivo induction of virulence and antibiotic
637 resistance transfer in *Enterococcus faecalis* mediated by the sex pheromone-sensing system
638 of pCF10. *Infection and Immunity* **70(2)**:716–723 DOI 10.1128/IAI.70.2.716.
- 639 **Hong H, Patel DR, Tamm LK, Van Den Berg B. 2006.** The outer membrane protein OmpW
640 forms an eight-stranded β -barrel with a hydrophobic channel. *Journal of Biological*
641 *Chemistry* **281(11)**:7568–7577 DOI 10.1074/jbc.M512365200.
- 642 **Huelsenbeck JP, Ronquist F. 2001.** MRBAYES: Bayesian inference of phylogenetic trees.
643 *Bioinformatics* **17(8)**:754–755 DOI 10.1093/bioinformatics/17.8.754.

- 644 **Kadowaki T, Yukitake H, Naito M, Sato K, Kikuchi Y, Kondo Y, Shoji M, Nakayama K.**
645 **2016.** A two-component system regulates gene expression of the type IX secretion
646 component proteins via an ECF sigma factor. *Scientific Reports* **6**:23288 DOI
647 10.1038/srep23288.
- 648 **Karlsson FH, Ussery DW, Nielsen J, Nookaew I.** **2011.** A closer look at Bacteroides:
649 phylogenetic relationship and genomic implications of a life in the human gut. *Microbial*
650 *Ecology* **61(3)**:473–485 DOI 10.1007/s00248-010-9796-1.
- 651 **Katoh K, Misawa K, Kuma KI, Miyata T.** **2002.** MAFFT: a novel method for rapid multiple
652 sequence alignment based on fast Fourier transform. *Nucleic Acids Research* **30(14)**:3059–
653 3066 DOI 10.1093/nar/gkf436.
- 654 **Khader YS, Dauod AS, El-Qaderi SS, Alkafajei A, Batayha WQ.** **2006.** Periodontal status of
655 diabetics compared with nondiabetics: a meta-analysis. *Journal of Diabetes and its*
656 *Complications* **20(1)**:59–68 DOI 10.1016/j.jdiacomp.2005.05.006.
- 657 **Kinane DF, Stathopoulou PG, Papapanou PN.** **2017.** Periodontal diseases. *Nature Reviews*
658 *Disease Primers* **3**:17038 DOI doi:10.1038/nrdp.2017.38.
- 659 **Lasica AM, Goulas T, Mizgalska D, Zhou X, De Diego I, Ksiazek M, Madej M, Guo Y,**
660 **Guevara T, Nowak M, Potempa B, Goel A, Sztukowska M, Prabhakar AT, Bzowska**
661 **M, Widziol M, Thøgersen IB, Enghild JJ, Simonian M, Kulczyk AW, Nguyen KA,**
662 **Potempa J, Gomis-Rüth FX.** **2016.** Structural and functional probing of PorZ, an essential
663 bacterial surface component of the type-IX secretion system of human oral-microbiomic
664 *Porphyromonas gingivalis*. *Scientific Reports* **6**:37708 DOI 10.1038/srep37708.
- 665 **Lasica AM, Ksiazek M, Madej M, Potempa J.** **2017.** The type IX secretion system (T9SS):
666 highlights and recent insights into its structure and function. *Frontiers in Cellular and*
667 *Infection Microbiology* **7**:215 DOI 10.3389/fcimb.2017.00215.
- 668 **Lauber F, Deme JC, Lea SM, Berks BC.** **2018.** Type 9 secretion system structures reveal a
669 new protein transport mechanism. *Nature* **564(7734)**:77 DOI 10.1038/s41586-018-0693-y.
- 670 **Laugisch O, Wong A, Sroka A, Kantyka T, Koziel J, Neuhaus K, Sculean A, Venables PJ,**
671 **Potempa J, Möller B, Eick S.** **2016.** Citrullination in the periodontium—a possible link
672 between periodontitis and rheumatoid arthritis. *Clinical Oral Investigations* **20(4)**:675–683
673 DOI 10.1007/s00784-015-1556-7.
- 674 **Letunic I, Bork P.** **2019.** Interactive Tree Of Life (iTOL) v4: recent updates and new
675 developments. *Nucleic Acids Research* **47(W1)**:W256–W259 DOI 10.1093/nar/gkz239.
- 676 **Li N, Zhu Y, LaFrentz BR, Evenhuis JP, Hunnicutt DW, Conrad RA, Barbier P,**
677 **Gullstrand CW, Roets JE, Powers JL, Kulkarni SS, Erbes DH, Garcia JC, Nie P,**
678 **McBride MJ.** **2017.** The type IX secretion system is required for virulence of the fish
679 pathogen *Flavobacterium columnare*. *Applied and Environmental Microbiology*
680 **83(23)**:e01769-17 DOI 10.1128/aem.01769-17.
- 681 **Mahillon J, Chandler M.** **1998.** Insertion sequences. *Microbiology and Molecular Biology*
682 *Reviews* **62(3)**:725–774
- 683 **Maresz KJ, Hellvard A, Sroka A, Adamowicz K, Bielecka E, Koziel J, Gawron K,**
684 **Mizgalska D, Marcinska KA, Benedyk M, Pyrc K, Quirke AM, Jonsson R, Alzabin S,**
685 **Venables PJ, Nguyen KA, Mydel P, Potempa J.** **2013.** *Porphyromonas gingivalis*
686 facilitates the development and progression of destructive arthritis through its unique
687 bacterial peptidylarginine deiminase (PAD). *PLoS Pathogens* **9(9)**:e1003627 DOI
688 10.1371/journal.ppat.1003627.
- 689 **McBride MJ, Zhu Y.** **2013.** Gliding motility and Por secretion system genes are widespread

- 690 among members of the phylum Bacteroidetes. *Journal of Bacteriology* **195(2)**:270–278 DOI
691 10.1128/JB.01962-12.
- 692 **Miller MA, Pfeiffer W, Schwartz T. 2010.** Creating the CIPRES Science Gateway for
693 inference of large phylogenetic trees. In: *Proceedings of the Gateway Computing*
694 *Environments Workshop (GCE)*. 1–8 DOI 10.1109/GCE.2010.5676129.
- 695 **Naas AE, Solden LM, Norbeck AD, Brewer H, Hagen LH, Heggenes IM, McHardy AC,**
696 **Mackie RI, Paša-Tolic L, Arntzen MØ, Eijsink VGH, Koropatkin NM, Hess M,**
697 **Wrighton KC, Pope PB. 2018.** “*Candidatus* Paraporphyromonas polyenzymogenes”
698 encodes multi-modular cellulases linked to the type IX secretion system. *Microbiome*
699 **6(1)**:44 DOI 10.1186/s40168-018-0421-8.
- 700 **Naito M, Tominaga T, Shoji M, Nakayama K. 2019.** PGN_0297 is an essential component of
701 the type IX secretion system (T9SS) in *Porphyromonas gingivalis*: Tn-seq analysis for
702 exhaustive identification of T9SS-related genes. *Microbiology and Immunology* **63(1)**:11–
703 20 DOI 10.1111/1348-0421.12665.
- 704 **Naito M, Hirakawa H, Yamashita A, Ohara N, Shoji M, Yukitake H, Nakayama K, Toh H,**
705 **Yoshimura F, Kuhara S, Hattori M. 2008.** Determination of the genome sequence of
706 *Porphyromonas gingivalis* strain ATCC 33277 and genomic comparison with strain W83
707 revealed extensive genome rearrangements in *P. gingivalis*. *DNA Research* **15(4)**:215–225
708 DOI 10.1093/dnares/dsn013.
- 709 **Nakane D, Sato K, Wada H, McBride MJ, Nakayama K. 2013.** Helical flow of surface
710 protein required for bacterial gliding motility. *Proceedings of the National Academy of*
711 *Sciences* **110(27)**:11145–11150 DOI 10.1073/pnas.1219753110.
- 712 **Nguyen KA, Zylicz J, Szczesny P, Sroka A, Hunter N, Potempa J. 2009.** Verification of a
713 topology model of PorT as an integral outer-membrane protein in *Porphyromonas*
714 *gingivalis*. *Microbiology (Reading, England)* **155(Pt 2)**:328 DOI 10.1099/mic.0.024323-0.
- 715 **Nikaido H. 2003.** Molecular basis of bacterial outer membrane permeability revisited.
716 *Microbiology and Molecular Biology Reviews* **67(4)**:593–656 DOI
717 10.1128/MMBR.67.4.593.
- 718 **Osbourn AE, Field B. 2009.** Operons. *Cellular and Molecular Life Sciences* **66(23)**:3755–3775
719 DOI 10.1007/s00018-009-0114-3.
- 720 **Pei AY, Oberdorf WE, Nossa CW, Agarwal A, Chokshi P, Gerz EA, Jin Z, Lee P, Yang L,**
721 **Poles M, Brown SM, Sotero S, DeSantis T, Brodie E, Nelson K, Pei Z. 2010.** Diversity
722 of 16S rRNA genes within Individual Prokaryotic Genomes. *Applied and Environmental*
723 *Microbiology* **76(12)**:3886–3897 DOI 10.1128/AEM.02953-09.
- 724 **Potempa J, Pike R, Travis J. 1995.** The multiple forms of trypsin-like activity present in
725 various strains of *Porphyromonas gingivalis* are due to the presence of either Arg-gingipain
726 or Lys-gingipain. *Infection and Immunity* **63(4)**:1176–1182
- 727 **Pylro VS, Vespoli LDS, Duarte GF, Yotoko KSC. 2012.** Detection of horizontal gene transfers
728 from phylogenetic comparisons. *International Journal of Evolutionary Biology* **2012** DOI
729 10.1155/2012/813015.
- 730 **Rahman MS, Simser JA, Macaluso KR, Azad AF. 2003.** Molecular and functional analysis of
731 the lepB gene, encoding a type I signal peptidase from *Rickettsia rickettsii* and *Rickettsia*
732 *typhi*. *Journal of Bacteriology* **185(15)**:4578–4584 DOI 10.1128/JB.185.15.4578-
733 4584.2003.
- 734 **Saiki K, Konishi K. 2010.** Identification of a novel *Porphyromonas gingivalis* outer membrane
735 protein, PG534, required for the production of active gingipains. *FEMS Microbiology*

- 736 *Letters* **310(2)**:168–174 DOI 10.1111/j.1574-6968.2010.02059.x.
- 737 **Sato K, Naito M, Yukitake H, Hirakawa H, Shoji M, McBride MJ, Rhodes RG, Nakayama**
738 **K. 2010.** A protein secretion system linked to bacteroidete gliding motility and
739 pathogenesis. *Proceedings of the National Academy of Sciences* **107(1)**:276–281 DOI
740 10.1073/pnas.0912010107.
- 741 **Schwarz G. 1978.** Estimating the dimension of a model. *The Annals of Statistics* **6(2)**:461–464
- 742 **Sela I, Ashkenazy H, Katoh K, Pupko T. 2015.** GUIDANCE2: Accurate detection of
743 unreliable alignment regions accounting for the uncertainty of multiple parameters. *Nucleic*
744 *Acids Research* **43(W1)**:W7–W14 DOI 10.1093/nar/gkv318.
- 745 **Shoji M, Sato K, Yukitake H, Kamaguchi A, Sasaki Y, Naito M, Nakayama K. 2018.**
746 Identification of genes encoding glycosyltransferases involved in lipopolysaccharide
747 synthesis in *Porphyromonas gingivalis*. *Molecular Oral Microbiology* **33(1)**:68–80 DOI
748 10.1111/omi.12200.
- 749 **Shoji M, Sato K, Yukitake H, Naito M, Nakayama K. 2014.** Involvement of the Wbp pathway
750 in the biosynthesis of *Porphyromonas gingivalis* lipopolysaccharide with anionic
751 polysaccharide. *Scientific Reports* **4**:5056 DOI 10.1038/srep05056.
- 752 **Shoji M, Yukitake H, Sato K, Shibata Y, Naito M, Aduse-Opoku J, Abiko Y, Curtis MA,**
753 **Nakayama K. 2013.** Identification of an O-antigen chain length regulator, WzzP, in
754 *Porphyromonas gingivalis*. *MicrobiologyOpen* **2(3)**:383–401 DOI 10.1002/mbo3.84.
- 755 **Shoji M, Ratnayake DB, Shi Y, Kadowaki T, Yamamoto K, Yoshimura F, Akamine A,**
756 **Curtis MA, Nakayama K. 2002.** Construction and characterization of a nonpigmented
757 mutant of *Porphyromonas gingivalis*: cell surface polysaccharide as an anchorage for
758 gingipains. *Microbiology* **148(4)**:1183–1191 DOI 10.1099/00221287-148-4-1183.
- 759 **Taguchi Y, Sato K, Yukitake H, Inoue T, Nakayama M, Naito M, Kondo Y, Kano K,**
760 **Hoshino T, Nakayama K, Takashiba S, Ohara N. 2016.** Involvement of an Skp-like
761 protein, PGN_0300, in the Type IX secretion system of *Porphyromonas gingivalis*.
762 *Infection and Immunity* **84(1)**:230–240 DOI 10.1128/IAI.01308-15.
- 763 **Thomas CM, Nielsen KM. 2005.** Mechanisms of, and barriers to, horizontal gene transfer
764 between bacteria. *Nature Reviews Microbiology* **3(9)**:711 DOI 10.1038/nrmicro1234.
- 765 **Vincent MS, Chabaliier M, Cascales E. 2018.** A conserved motif of Porphyromonas Type IX
766 secretion effectors C-terminal secretion signal specifies interactions with the PorKLMN
767 core complex. *BioRxiv*:483123 DOI 10.1101/483123.
- 768 **Vincent MS, Canestrari MJ, Leone P, Stathopoulos J, Ize B, Zoued A, Cambillau C,**
769 **Kellenberger C, Roussel A, Cascales E. 2017.** Characterization of the *Porphyromonas*
770 *gingivalis* type IX secretion trans-envelope PorKLMNP core complex. *Journal of*
771 *Biological Chemistry* **292(8)**:3252–3261 DOI 10.1074/jbc.M116.765081.
- 772 **Winker S, Woese CR. 1991.** A Definition of the Domains Archaea, Bacteria and Eucarya in
773 Terms of Small Subunit Ribosomal RNA Characteristics. *Systematic and Applied*
774 *Microbiology* **14(4)**:305–310 DOI 10.1016/S0723-2020(11)80303-6.
- 775 **Yanofsky C, Lennox ES. 1959.** Transduction and recombination study of linkage relationships
776 among the genes controlling tryptophan synthesis in *Escherichia coli*. *Virology* **8(4)**:425–
777 447 DOI 10.1016/0042-6822(59)90046-7.

Figure 1

T9SS protein components on the inner membrane (IM) and outer membrane (OM) of *Porphyromonas gingivalis*.

The protein components with known functions are represented by coloured structures. The pathway for cargo protein gingipain (RgpB) translocation and modifications by T9SS is illustrated. The regulation of the pathway by the protein components is also exhibited.

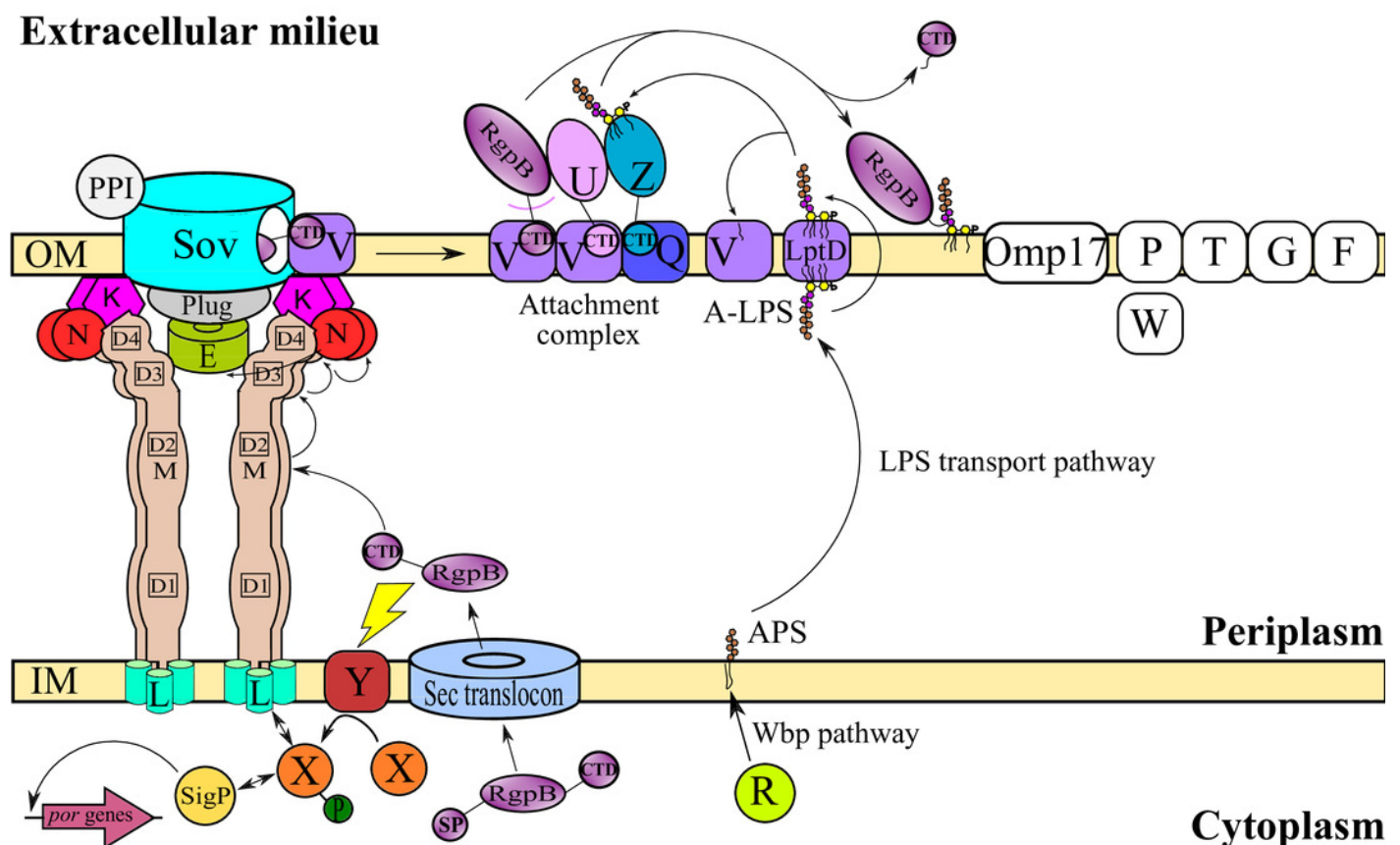


Figure 2

The Bayesian Inference (BI) phylogenetic trees of T9SS protein components (PorK, PorL, PorM, and PorN).

(A) BI tree of PorK. (B) BI tree of PorL. (C) BI tree of PorM. (D) BI tree of PorN. The terminal nodes are labelled with coloured circles that represent the classes under Bacteroidetes that each protein homolog belongs to. The classes represented by each colour are provided in the legend inside the figure. The branches with strong support (posterior probability value > 0.95) are coloured in black. Otherwise, the branches are coloured in red. The solid curve denotes a monophyletic clade that formed by terminal nodes that belong to the same class under Bacteroidetes. The dashed curve denotes a strong support for the monophyletic clade or its subclade. The colour of curve represents the class of terminal nodes that form the clade. The classes represented by each colour are shown in the legend inside the figure.

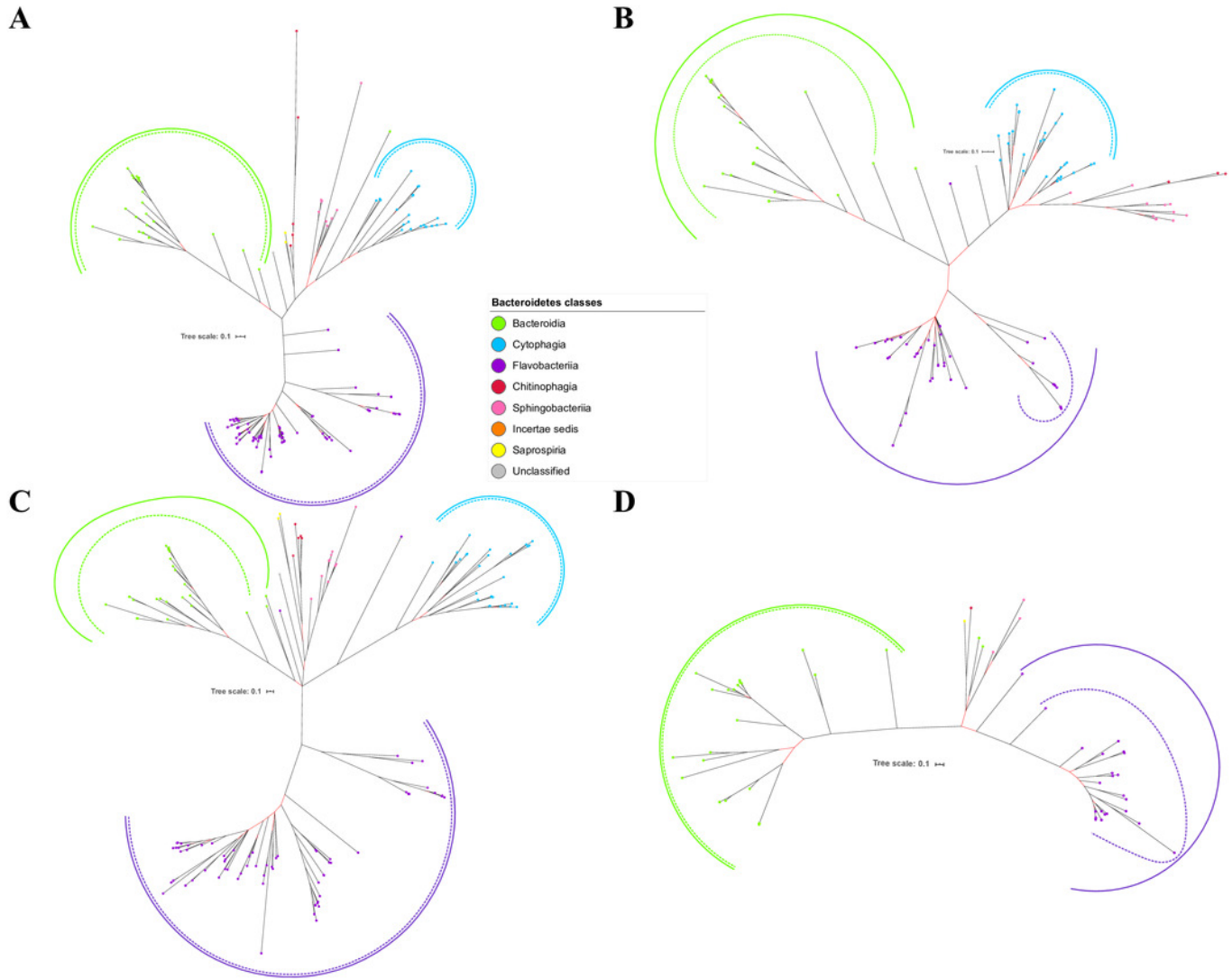


Figure 3

The Bayesian Inference (BI) phylogenetic trees of T9SS protein components (PorP, PorQ, PorR, and Sov).

(A) BI tree of PorP. (B) BI tree of PorQ. (C) BI tree of PorR. (D) BI tree of Sov.

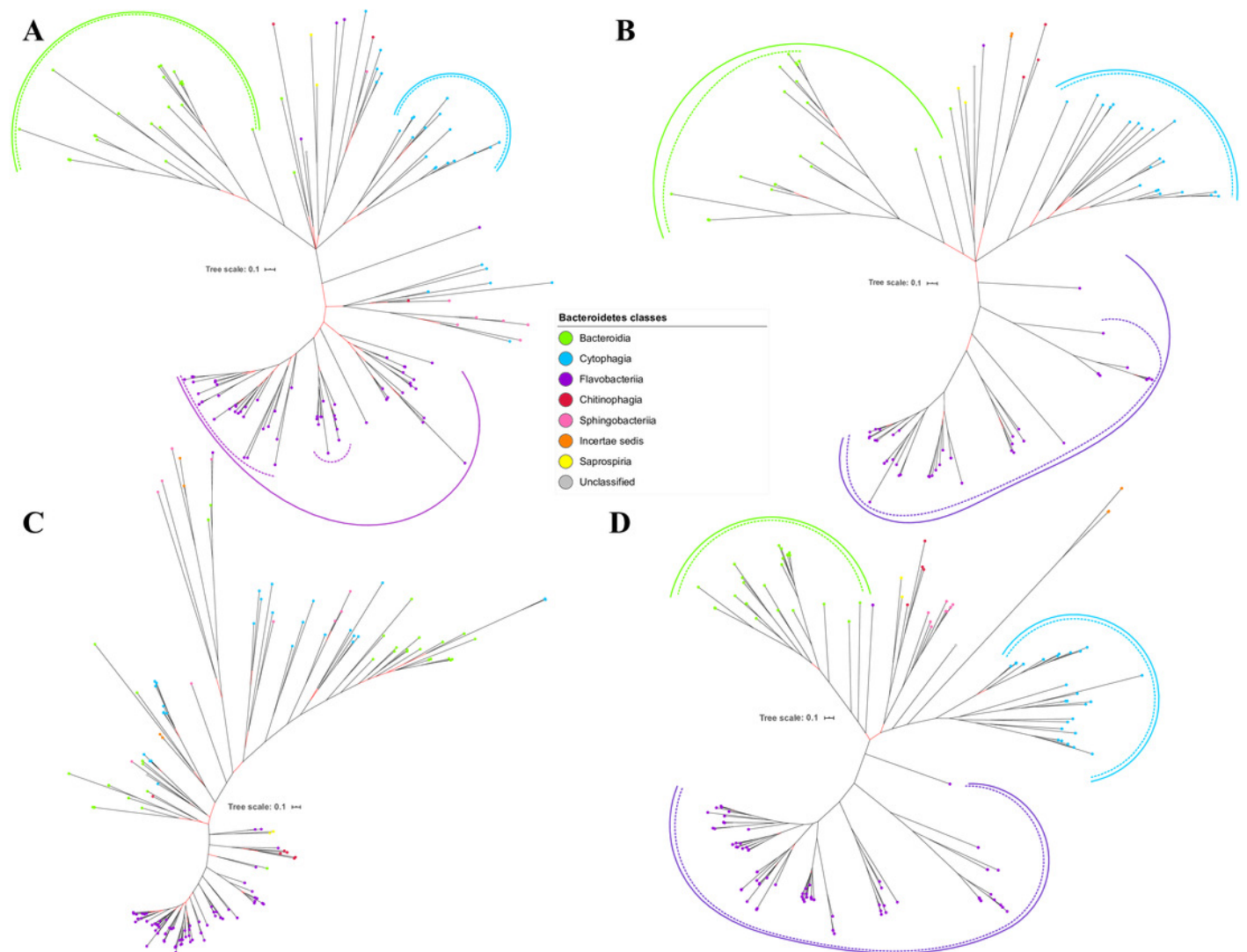


Figure 4

The Bayesian Inference (BI) phylogenetic trees of T9SS protein components (PorT, PorU, PorV, and PorW).

(A) BI tree of PorT. (B) BI tree of PorU. (C) BI tree of PorV. (D) BI tree of PorW.

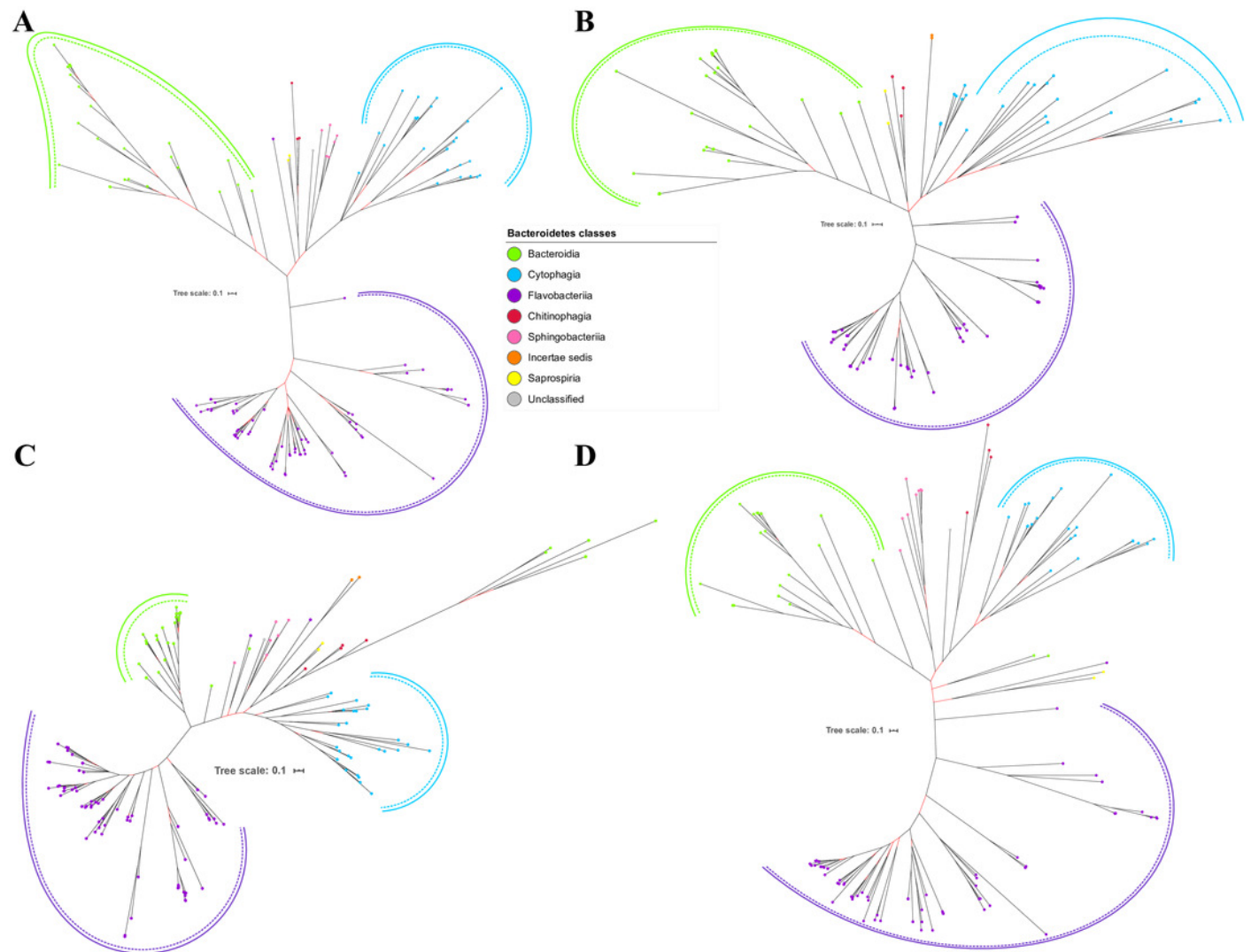


Figure 5

The Bayesian Inference (BI) phylogenetic trees of T9SS protein components (PorX, PorY, PorZ, and SigP).

(A) BI tree of PorX. (B) BI tree of PorY. (C) BI tree of PorZ. (D) BI tree of SigP.

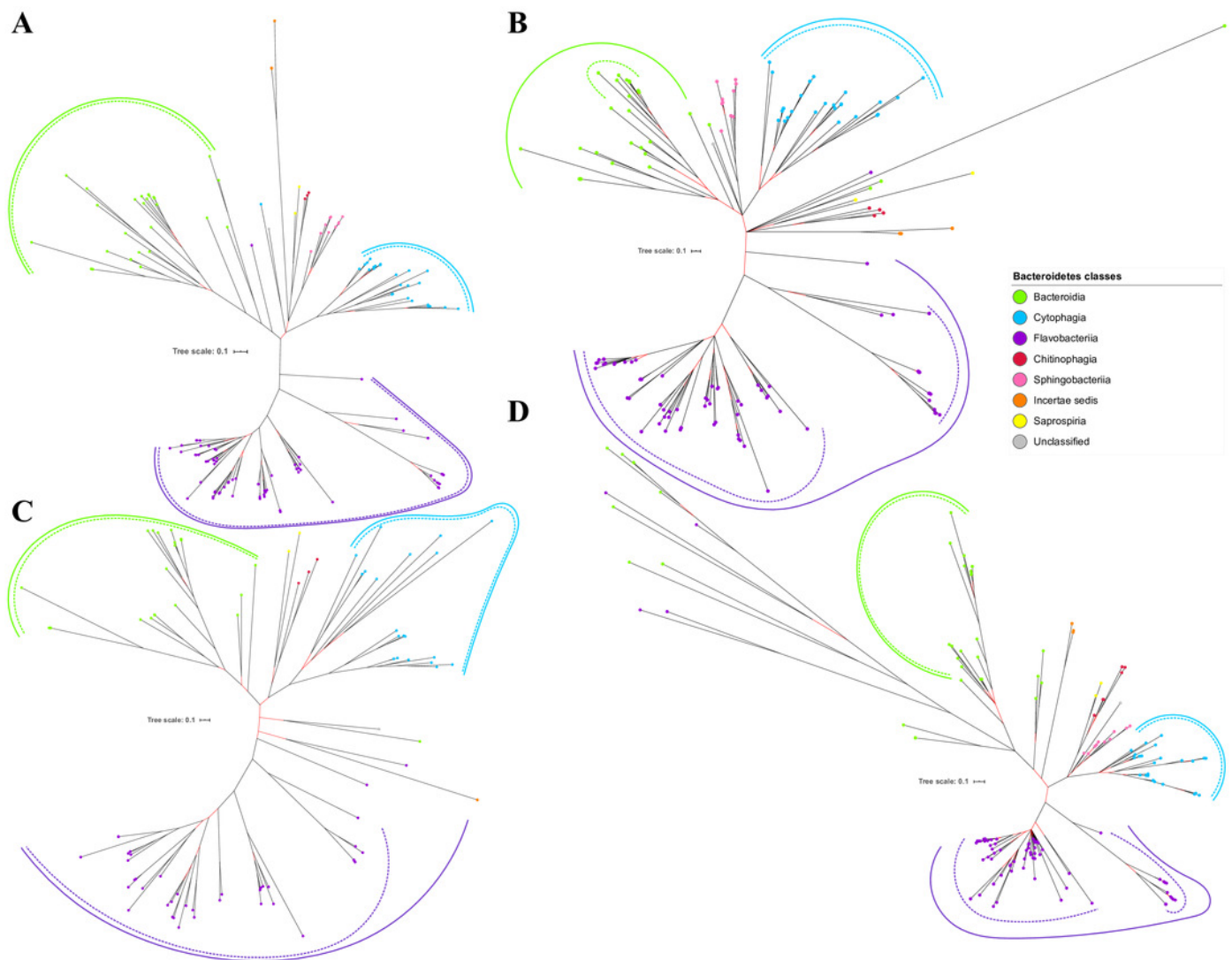


Figure 6

The Bayesian Inference (BI) phylogenetic trees of T9SS protein components (Omp17, PorE, PorF, and PorG).

(A) BI tree of Omp17. (B) BI tree of PorE. (C) BI tree of PorF. (D) BI tree of PorG.

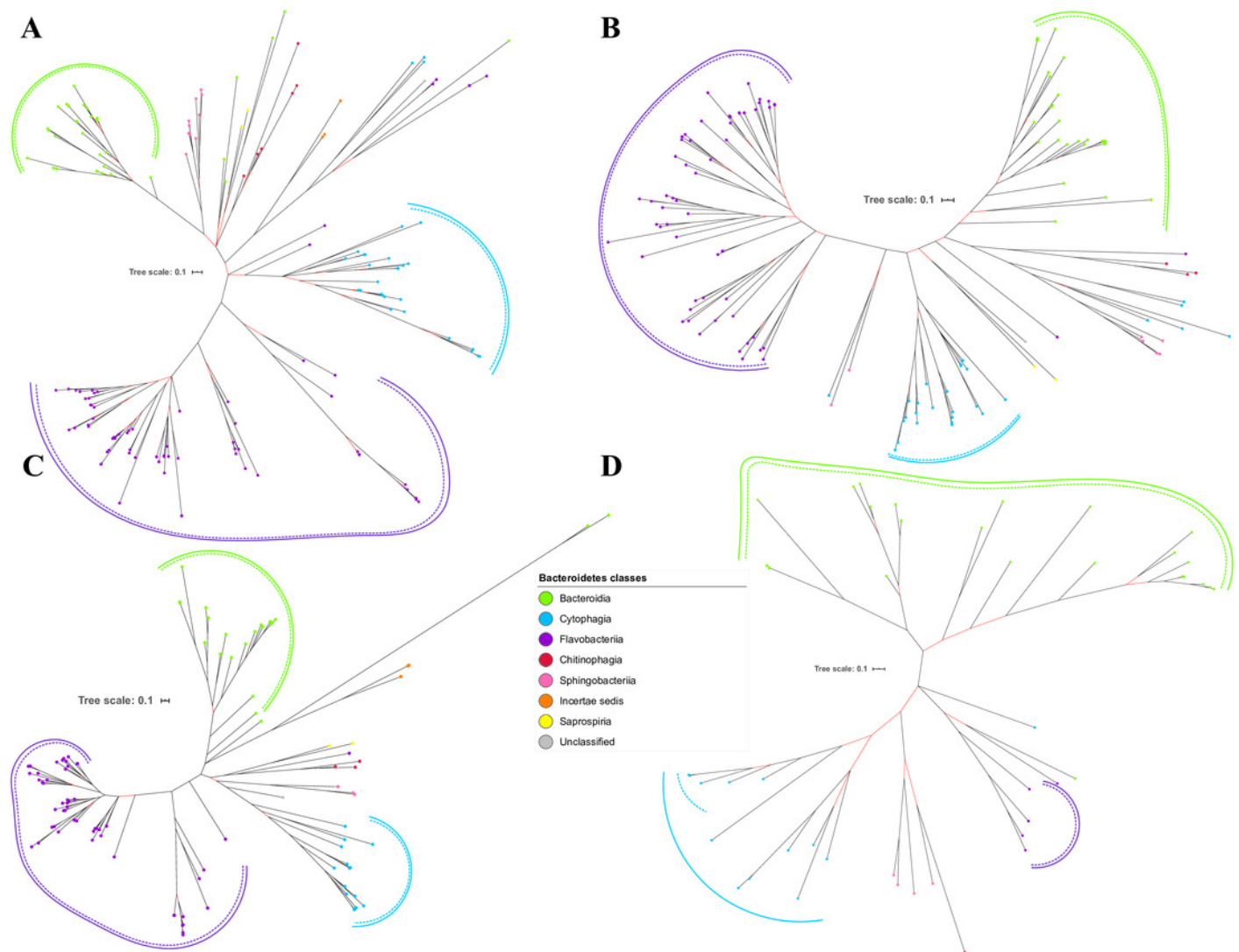


Figure 7

The Bayesian Inference (BI) phylogenetic tree of 16S ribosomal RNA (rRNA).

The BI tree of 16S rRNA exhibits monophyletic clades where each clade consists of terminal nodes of the same colour that denotes that they belong to the same class under Bacteroidetes. There is a high support (posterior probability value > 0.95) for each monophyletic clade indicated by the black branch leading to each clade. The solid and dashed green, purple, and blue curves indicate there is a strong support for the monophyletic clades of Bacteroidia, Flavobacteriia, and Cytophagia classes respectively.

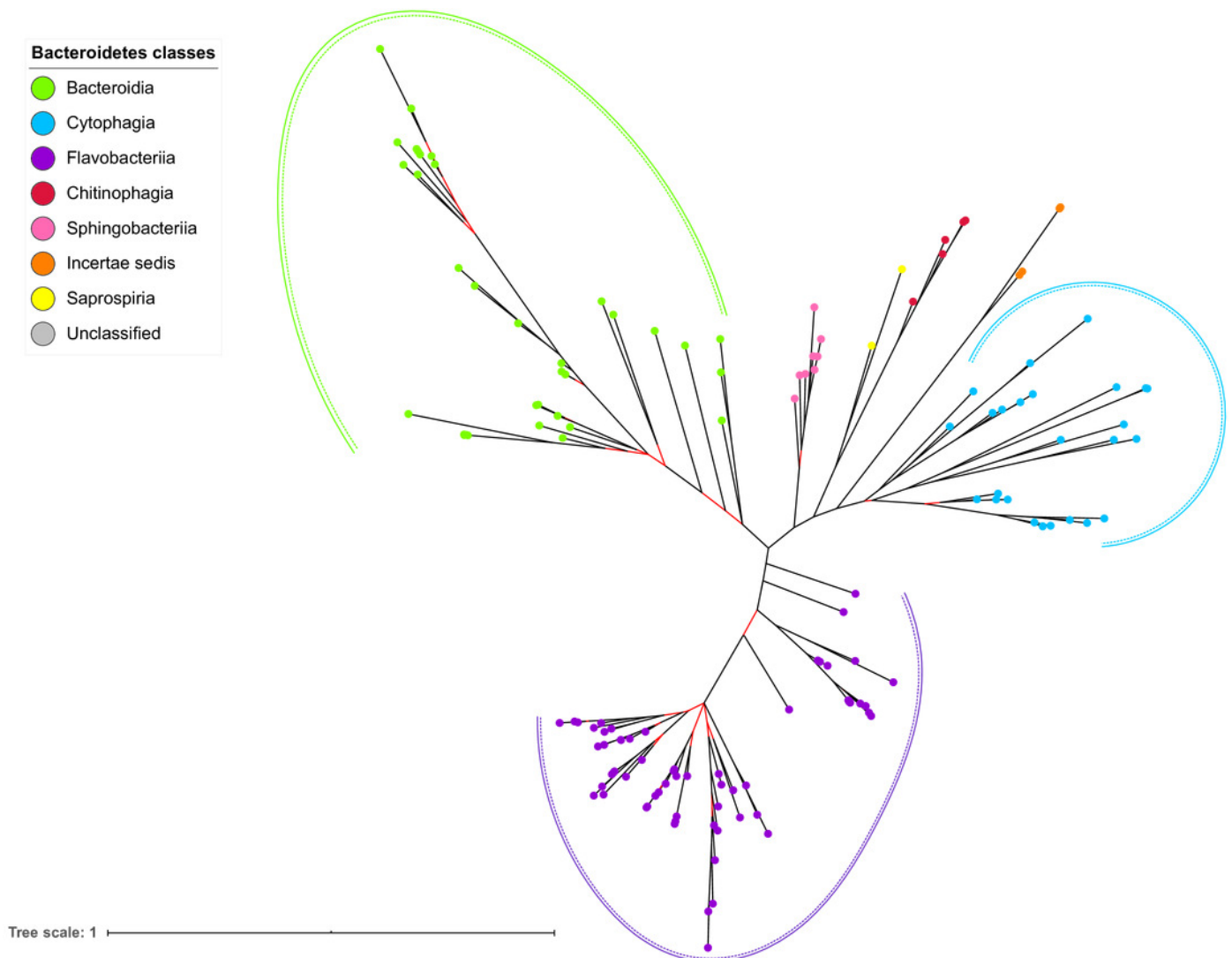


Figure 8

The arrangement of *porR* and its neighbouring genes in *P. gingivalis* ATCC 33277 genome.

porR (PGN_1236) and its neighbouring genes are flanked by IS5 family transposons that formed a composite transposon of 70 kbp in length. The genes that involve in biosynthesis of A-LPS are represented by yellow rectangles while the gene that does not involve is represented by brown rectangle. The genes for hypothetical proteins are represented by white rectangles. The genes for IS5 family transposases are represented by cyan rectangles. The purple triangles represented 12 bp inverted repeats that flanked the genes for IS5 family transposases. Name of proteins encoded by the genes are shown under rectangles that represented the genes. The slashes indicated gaps in the genome.

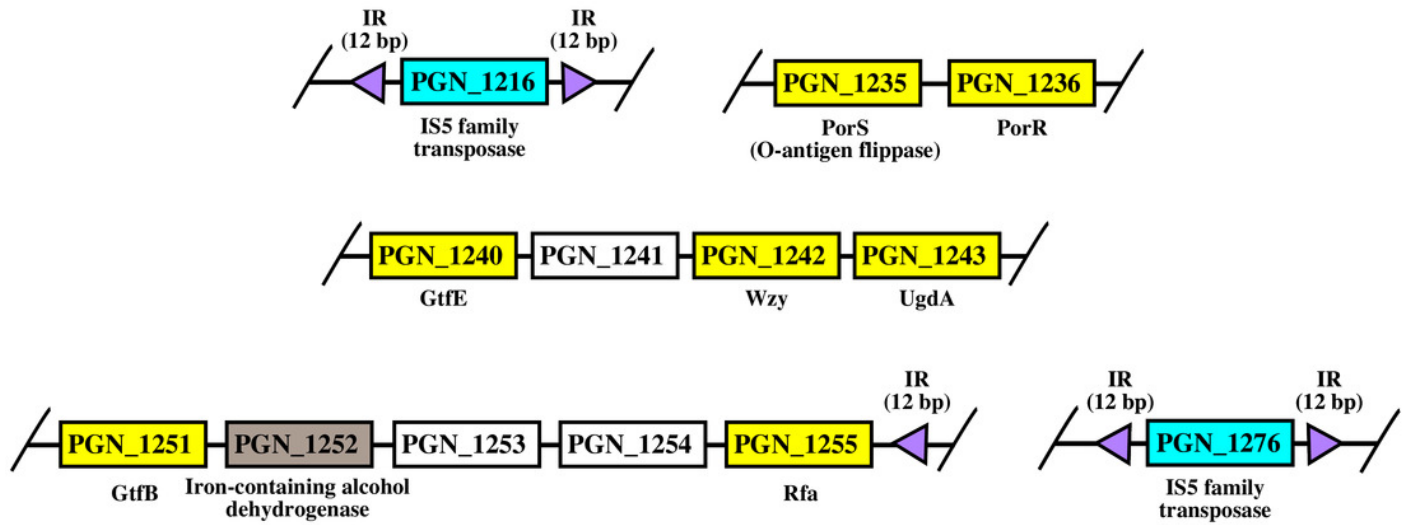


Figure 9

Comparison between the Bayesian Inference (BI) tree of UgdA with BI tree of PorR.

The BI tree of UgdA (A) does not exhibit monophyletic clades for all major classes under Bacteroidetes which is similar to the BI tree of PorR (B). Both BI trees of UgdA and PorR also exhibit similar topology. Both trees exhibit cluster I (solid purple curve) that primarily consists of terminal nodes of Flavobacteriia and a few terminal nodes from other classes. Both trees have cluster II (solid green curve) that consists of terminal nodes of Porphyromonas, Tannerella, and Parabacteroides genera. Both trees acquire cluster III (solid blue curve) that consists of terminal nodes of Rufibacter and Hymenobacter genera. Both trees exhibit cluster IV (solid green curve) that consists of terminal nodes of Prevotella, Bacteroides, Proteiniphilum, and other genera.

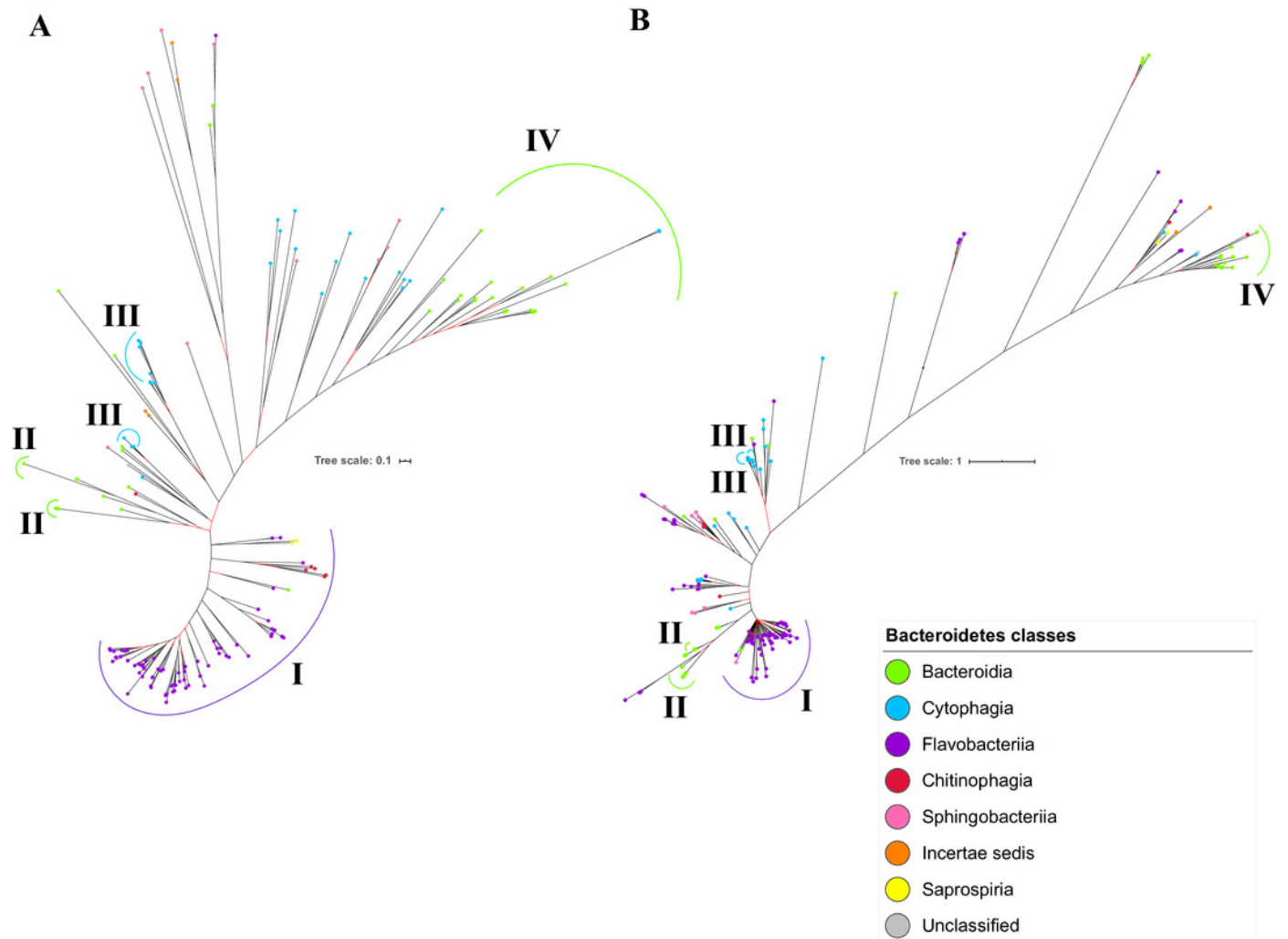


Figure 10

The species from Chitinophagia, Saprospira, and unclassified under Bacteroidetes phylum that acquired homologs of T9SS protein components.

The colours of rectangles denote the classes those species belong to. Coloured squares indicate T9SS component homologs acquired by the species where the different colours denote different functions those components performed. White squares indicate T9SS component homologs absent in those species.

Species	PapK	PapL	PapM	PapY	PapP	PapQ	PapR	Sap	PapT	PapU	PapV	PapW	PapX	PapY	PapZ	SigP	Omp17	PapE	PapF	PapG
<i>Halicomonobacter hydrossis</i> DSM1100	Blue	White	Blue	Blue	Grey	Green	Orange	Blue	Grey	Green	Green	Grey	Red	Red	Green	Red	Grey	Blue	Grey	White
<i>Saprospira grandis</i> str. Lewin	Blue	White	Blue	White	Grey	Green	Orange	Blue	Grey	Green	Green	Grey	Red	Red	Green	Red	Grey	Blue	Grey	White
<i>Niastella koreensis</i> GR20-10	Blue	Blue	Blue	Blue	Grey	Green	Orange	Blue	Grey	Green	Green	Grey	Red	Red	Green	Red	Grey	Blue	Grey	White
<i>Flavisolibacter</i> sp. LCS9	Blue	Blue	Blue	White	Grey	Green	Orange	Blue	Grey	Green	Green	Grey	Red	Red	Green	Red	Grey	Blue	Grey	White
<i>Niabella ginsenosidivorans</i>	Blue	White	Blue	White	Grey	White	Orange	White	Grey	White	White	White	White	White	White	Red	Grey	White	White	White
<i>Arachidococcus</i> sp. BS20	Blue	White	Blue	White	Grey	White	Orange	Blue	Grey	Green	Green	Grey	White	Red	White	Red	Grey	White	White	White
<i>Chitinophaga pinensis</i> DSM 2588	Blue	Blue	Blue	White	Grey	Green	Orange	Blue	Grey	White	Green	Grey	Red	Red	Green	Red	Grey	Blue	Grey	White
Bacteroidetes bacterium UKL13-3	Blue	Blue	Blue	White	Grey	Green	Orange	Blue	Grey	White	Green	Grey	Red	Red	Green	Red	Grey	Blue	Grey	White

Legend

- Red: Regulation
- Blue: Translocation & Energetic
- Green: Modification
- Orange: A-LPS biosynthesis
- Grey: Unknown
- Yellow: Saprospira
- Pink: Chitinophagia
- Dark Grey: Unclassified

Table 1 (on next page)

The characteristics of T9SS component protein alignments and the best amino acid substitution models that have been selected for them.

The characteristics of T9SS component protein alignments such as no. of taxa used to construct the alignments and no. of characters of the alignments are provided. The best amino acid substitution model that has been selected for each alignment is also provided. The definition of parameters of the best amino acid substitution models are provided in the footnote.

Alignment	No. of taxa	No. of characters	Model
Omp17	180	245	LG + G + F
PorE	137	793	LG + G + I
PorF	121	829	LG + G + I + F
PorG	55	487	LG + G + I
PorK	153	561	LG + G + I
PorL	123	281	LG + G + I
PorM	159	406	LG + G + I + F
PorN	62	267	LG + G + I
PorP	138	281	LG + G + I + F
PorQ	108	358	LG + G + F
PorR	176	471	LG + G + I
PorT	151	202	LG + G + F
PorU	109	919	LG + G + I
PorV	162	360	LG + G + I + F
PorW	137	995	LG + G + I + F
PorX	162	624	LG + G + I
PorY	162	897	LG + G + I
PorZ	102	569	LG + G + I
SigP	177	197	LG + G + I
Sov	159	2704	LG + G + I + F
UgdA	176	460	LG + G + I
16S rRNA	144	1452	GTR + G + I

Note:

- LG + G: LG substitution model matrix with gamma-shaped rate variation across sites and Dirichlet stationary amino acid frequencies
- LG + G + I: LG substitution model matrix with gamma-shaped rate variation across sites with a proportion of invariable sites and Dirichlet stationary amino acid frequencies
- LG + G + I + F: LG substitution model matrix with gamma-shaped rate variation across sites with a proportion of invariable sites and fixed (empirical) stationary amino acid frequencies
- LG + G + F: LG substitution model matrix with gamma-shaped rate variation across sites and fixed (empirical) stationary amino acid frequencies
- GTR + G + I: General Time Reversible (GTR) substitution model matrix with gamma-shaped rate variation across sites with a proportion of invariable sites and Dirichlet stationary nucleotide frequencies

1
2
3
4
5
6
7
8
9
10
11
12
13
14